# Accepted Manuscript


Synthesis and biological activities of carbonyl cobalt CORMs with selectively inhibiting cyclooxygenase-2

Jili Li, Jinlong Zhang, Qiuping Zhang, Zhongjie Bai, Quanyi Zhao, Zhen Wang, Yonglin Chen, Bin Liu

PII: S0022-328X(18)30450-9

DOI: 10.1016/j.jorganchem.2018.08.013

Reference: JOM 20540

To appear in: *Journal of Organometallic Chemistry*

Received Date: 4 June 2018

Revised Date: 1 August 2018

Accepted Date: 14 August 2018

Please cite this article as: J. Li, J. Zhang, Q. Zhang, Z. Bai, Q. Zhao, Z. Wang, Y. Chen, B. Liu, Synthesis and biological activities of carbonyl cobalt CORMs with selectively inhibiting cyclooxygenase-2, *Journal of Organometallic Chemistry* (2018), doi: 10.1016/j.jorganchem.2018.08.013.

# Synthesis and biological activities of carbonyl cobalt CORMs with selectively inhibiting cyclooxygenase-2

Jili Li [a], Jinlong Zhang [a], Qiuping Zhang [a], Zhongjie Bai[a], Quanyi Zhao [a *], Zhen Wang [a], Yonglin Chen [b], Bin Liu [c]

*(a Institute of Medicinal Chemistry, School of Pharmacy of Lanzhou University; b The First Affiliated Hospital of Lanzhou University; c School of Stomatology of Lanzhou University, Lanzhou 730000, China)*

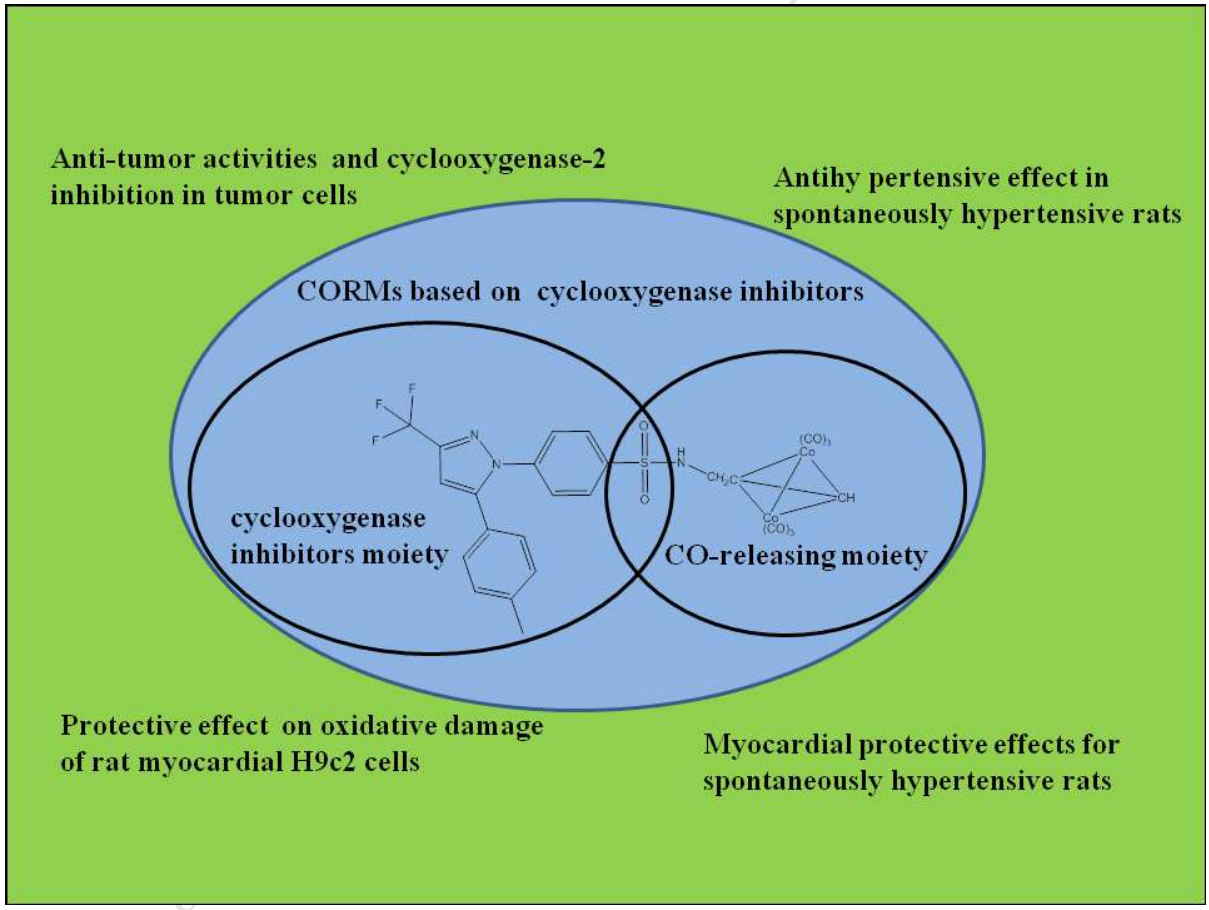


* Corresponding author. Tel.: +869318915686; fax: +869318915686.
E-mail address: zhaoqy@lzu.edu.cn

# Synthesis and biological activities of carbonyl cobalt CORMs with selectively inhibiting cyclooxygenase-2

Jili Li [a], Jinlong Zhang [a], Qiuping Zhang [a], Zhongjie Bai[a], Quanyi Zhao [a *], Zhen Wang [a], Yonglin Chen [b], Bin Liu [c]

*(a Institute of Medicinal Chemistry, School of Pharmacy of Lanzhou University; b The First Affiliated Hospital of Lanzhou University; c School of Stomatology of Lanzhou University, Lanzhou 730000, China)*

**Abstract:**

In this paper, three kinds of hybrid carbonyl cobalt CO-releasing molecules (CORMs), $RCOOCH_2C_2H[Co_2(CO)_6]$ (R=NSAIDs-COOH, **1-11**; R= celecoxib derivative-COOH, **15**), $RSO_2(R')\ CH_2C_2H[Co_2(CO)_6]$ (R= celecoxib, **12**; R= nimesulide, **13**) and $ROCH_2C_2H[Co_2(CO)_6]$ (R= ferulic acid etheyl ester, **14**), were synthesized and characterized by IR, NMR and HRMS. The crystal structures of complexes **9**, **11**, **14** and **16** were determined by single-crystal X-ray diffraction. Meanwhile, the anti-tumor activity, protection on oxidative damage of H9c2 cells, anti-hypertension and myocardial protective effects were evaluated. The results showed only a part of the complexes had anticancer activity for the five cell lines compared with 5-FU. Among them, complexes **12** and **13** which modified by selective COX-2 inhibitors displayed strong antiproliferative activity and selectivity to MCF-7 cell and HT-29 cell lines, and their $IC_{50}$ values were 33.6-55.8 μM; but compared with cis-platin (DDP), they showed slightly lower activities. The complex inhibited the expression of COX-2 in HT-29 cells and MCF-7cells, and complex **12** had stronger inhibitory effects than the others, which was accordance with its stronger activity against cell proliferation. Secondly, the complex improved the survival rate of H9c2 cells injured by $H_2O_2$. For each tested complex, the survival rate increased obviously after the cells treated with $H_2O_2$ for 1h; but it increased slowly when the cells harmed for 8h due to the severe cell injury. In addition, the complexes displayed antihypertensive effects on spontaneously hypertensive rats, accompanying with good myocardium protection. This indicates these hybrid CORMs reduced myocardial toxicity of COX-2 inhibitors like, but there still has liver and kidney side-effects when administrating continuously for 14 days.

* Corresponding author. Tel.: +869318915686; fax: +869318915686.
E-mail address: zhaoqy@lzu.edu.cn

**Key words:** carbonyl metal; CO-releasing molecule; cyclooxygenase-2; antihypertensive; myocardial protective effects

**1. Introduction**:

Carbon monoxide (CO) has drawn considerable attention because of its unexpected role in numerous physiological processes. [1] It was found to be beneficial in therapeutic applications such as systemic pulmonary hypertension, cardiac, renal, and small bowel graft rejections, as well as intestine disease, hemorrhagic shock, and lung injury. [2] Recently, the researcher found CO was directly related to tumor angiogenesis, [3] tumor cell energy metabolism [4] and immune regulation [5], which indicates CO has a big potential in clinic. But CO is a gas and uncontrollable dose and un-convenient use. Motterlini first used carbonyl metal CO releasing molecules (CORMs) as CO substitute, and confirmed CORMs had the same function as endogenous CO. [1, 6] After that, many carbonyl metal CORMs appeared, involving in metal Ru, Fe, Mn, Co, Mo, and so on. [7, 8–11]

Among all kinds carbonyl metal complexes, CORMs containing cobalt was focused on earlier. In 2005, Ott et al found many cobalt carbonyl complexes inhibited tumor cell proliferation, and their activities were connected with the structures of non-CO ligands; [12] Among these complexes, hexacarbonyl-[2-propinylacetyl salicylate] dicobalt was more active than cis-platin on the human mammary tumor cell lines MCF-7 and MDA-MB-231.[13-14] Hexacarbonyl-[ethinylestradiol] dicobalt complex was effective to hormone dependent tumors. [15] The cobalt carbonyl complexes not only displayed ant-cancer activity, but also had anti-inflammation. In following years, the researcher found their anti-inflammatory effects owed to liberating CO to inhibit nitrite, [16] and the effects of proliferative inhibition for cancer cells were mainly resulting from the CO to inhibit Hsp90 downstream protein activity, such as Akt, ER alpha, and cyclin D1; [17] the complexes also promoted apoptosis, disturbed cell cycle and interfered NDA synthesis by cobalt fragments [18].

Why the CORMs based on acetylsalicylic acid displayed better anti-proliferative activity to cancer cells, like MCF-7 and MDA-MB-231. With in-depth research on cancer, many evidences demonstrate inducible cyclooxygenase (COX-2) played an important role in tumorigenesis, development and metastasis of cancer. The proliferation of tumor cells accompanies with occurrence of inflammation in tumor development process. [19-20] COX-2 was over-expression in thyroid cancer, endometrial cancer and colon cancer, [21-22] and it was involved in tumor invasion, lymph node metastasis and clinical staging in non-small cell lung cancer. The expression of COX-2 was not only related to tumor size, postoperative pathology and expression of hypoxia inducible factor [23], but also participated in tumor resistance

through a variety of mechanisms. Acetylsalicylic acid cobalt carbonyl complexes on the proliferation of cancer cells inhibition maybe was related to the inhibition of COX-2 activity.

Considering the COX-2 roles in tumorigenesis and development process, metal carbonyl CORMs based on COX-2 inhibitor may play the dual effects, on the one hand, through cyclooxygenase pathway, inhibit tumor cell growth indirectly, reduce or weaken tumor development and metastasis; on the other hand, ROS and metal fragments produced by CORMs directly killing tumor cells. This kind of hybrid CORMs is likely to be a new kind anticancer agent. In addition, non-steriod anti-inflammatory drugs (NSAIDs), nimesulide and celecoxib are selective COX-2 inhibitors which were withdrawn from market due to myocardiotoxicity. Modified with CORMs, they will possibly overcome these flaws by CO biological function.

Therefore, on the basis of the above, we synthesized a kind of hybrid CORMs based on non-steriod anti-inflammatory drugs (NSAIDs), and evaluated biological function through their anti-tumor activities and regulation of COX-2 expression level; At the same time, we wonder whether CORMs improve selective COX-2 inhibitors side-effects through evaluating protective effect on oxidative damage of rat myocardial H9c2 cells, myocardial protective effects and antihypertensive effect. By which, we hope to provide a theoretical basis for the development of new drugs.

## 2. Results and discussion

### 2.1 Design, syntheses and properties of the complexes

Non-steroidal anti-inflammatory drugs (NSAIDs) are COX inhibitors which widely applied all over the world; many testing results show they not only have preventive and anticancer effects.[24-31] but also increase the activity of certain anticancer drugs when applied in combination[32-39]. Therefore, based on our previous work about CORMs, the structural fragments of compounds $A_{1-13}$ (Scheme 1, 2) were introduced into complexes **1-15** because of their activities, among them, $A_1$ –$A_{11}$ are nonselective COXIBs, which are NSAIDs in clinic. $A_8$ and $A_{14}$ have antithrombotic activity; $A_{12}$ and $A_{13}$ are selective COX-2 inhibitors which regrettably pulled off the market due to the cardiovascular toxicity. Considering carbonyl cobalt CORMs protecting cardiovascular effects, the combination of both COXIs and CORMs maybe overcome their side-effects and even have synergistic action. At the same time, $A_{1-14}$ can make the corresponding complex target specific organs and tissues, and possess stronger functions in vivo by primary metabolism.

Complexes **1-11** were prepared through the addition reaction of intermediates and $Co_2(CO)_8$; and $M_{1-11}$ were synthesized by the reactions of between organic acids with anti-inflammation and propargyl alcohol; complexes **12** and **13** were synthesized by replacing H atom of $NHSO_2$ group in nimesulide and celecoxib structures with

propargyl respectively on the alkaline condition, and then esterification; celecoxib has two H atom on $NH_2SO_2$ group, disubstituted product（complex **16**）was formed more easily; Complex **14** was prepared by the reaction of ferulic acid etheyl ester with propargyl bromide in the presence of potassium carbonate; complex **15** was afforded by the oxidation of methyl on celecoxib structure with potassium permanganate, and then esterification. The structures and synthetic routes for complexes **1-15** are shown in scheme 1and 2.

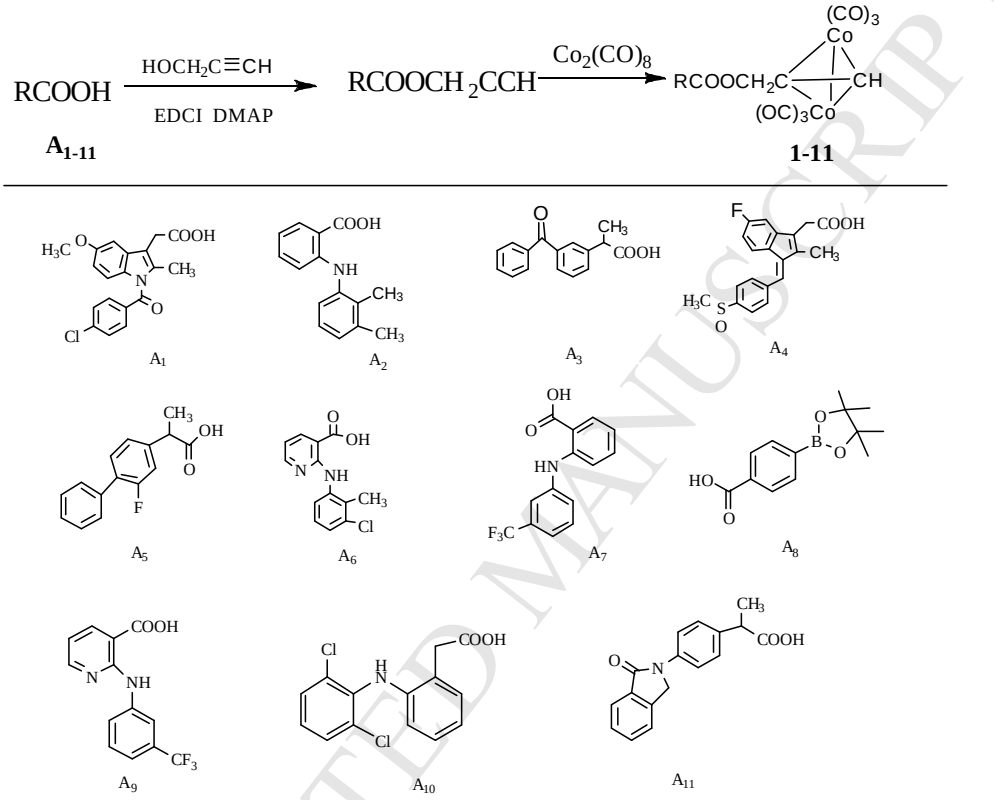


**Scheme 1** The structures and synthetic routes for complexes **1-11**

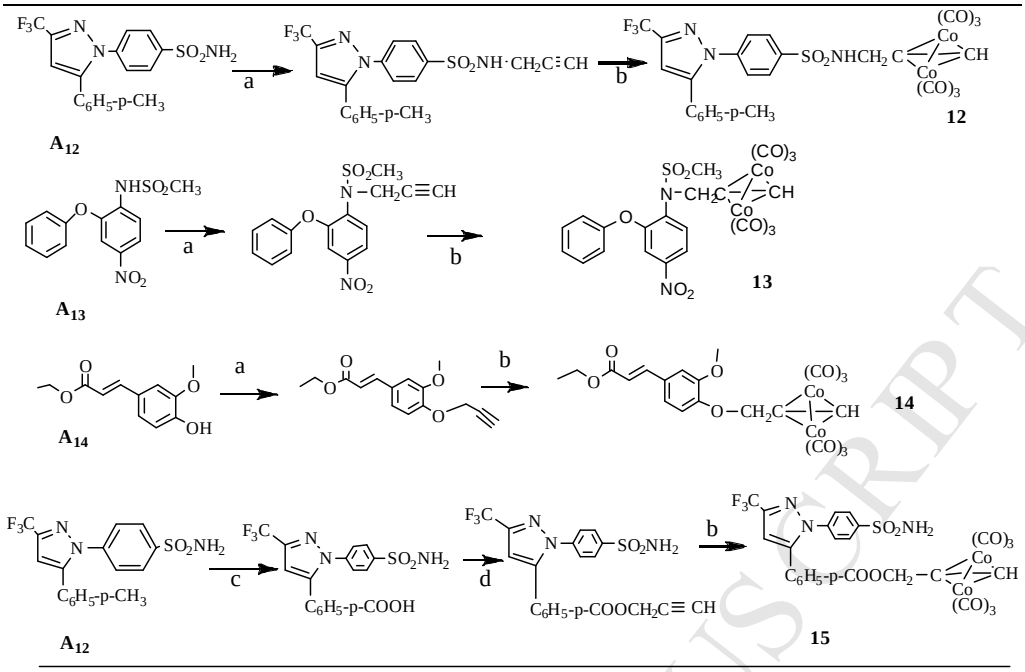


Reagents and conditions: a, propargyl bromide, $K_2CO_3$; b, $Co_2(CO)_8$; c, $KMnO_4$; d, propiolic alcohol, EDCI, DMAP

**Scheme 2** The structures and synthetic routes for complexes **12-15**

All complexes were characterized by a combination of NMR, ESI-HRMS and IR spectroscopy. All the complexes are red-black oils or red solids, stable in air for several days. They are insoluble in water, and easily dissolve in organic solvent. In the range of 2100–1996 $cm^{-1}$ appeared several strong terminal carbonyl absorptions in their IR spectra. The higher absorption bands were attributed to terminal carbonyls which coordinated to the Co atom. The IR spectra showed corresponding ester carbonyl absorptions at 1682–1736 $cm^{-1}$ for all the complexes except complexes **12** **13**,and **15**. In the $^1H$ NMR spectra of the complexes **12** and **15**, the chemical shifts of the parazole ring protons were observed at 6.67–6.79 ppm, signals at 5.26 ppm as singlet were assigned to hydrogen of $OCH_2$.

In addition, the crystal structures of complexes **9**, **11**, **14** and **16** were determined by single-crystal X-ray diffraction, their molecular structures are shown in Fig. 1. The details of the data collection and structure refinement are listed in Table 1. All four complexes but **16** have a common tetrahedral framework containing two cobalt atoms, different side chains make the Co-Co bond lengths changing slightly. For complex **16**, there have two tetrahedral frameworks containing $[Co_2(CO)_6]$ units to connect together through $–CH_2NCH_2-$ group; distinctly, the bond angle of C-N-C (119.2°) is much bigger than the normal angle of $sp^3$ hybrid N atom, and two fragments of $[Co_2(CO)_6]$ are away from each other as far as possible due to steric hindrance; For celecoxib fragment part, two benzene rings and a parazole ring are not in a plane

because of the effect of $[Co_2(CO)_6]$, two benzene rings are on both side of the plane of parazole ring. Their torsion angles are about 140.

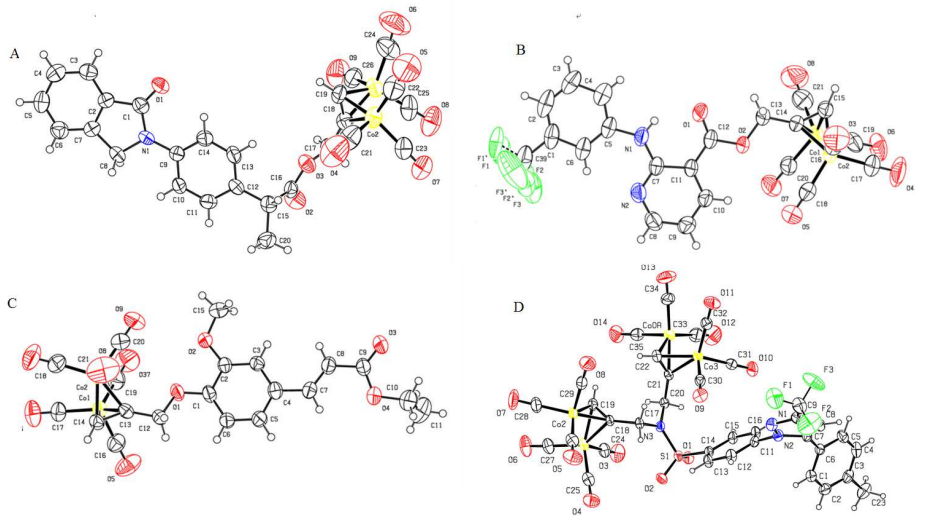

**Fig.1** The crystal structures of complexes**:** A for **11**, B for **9**, C for **14**, D for **16.**

**Table 1** Details of the data collection and structure refinement

| Complex | **A** | **B** | **C** | **D** |
|---|---|---|---|---|
| Formula | $C_{26}H_{17}Co_2NO_9$ | $C_{22}H_{11}Co_2F_3N_2O_8$ | $C_{21}H_{16}Co_2O_{10}$ | $C_{35}H_{18}Co_4F_3N_3O_{14}S$ |
| Formula weight | 605.27 | 606.19 | 546.20 | 1029.30 |
| Crystal system | monoclinic | monoclinic | monoclinic | monoclinic |
| Dimensions($mm^3$) | 0.21 × 0.15 × 0.14 | 0.25 × 0.24 × 0.17 | 0.19 × 0.07 × 0.05 | 0.25 × 0.07 × 0.04 |
| Space group | $P2_1/c$ | $P2_1/c$ | $P2_1/c$ | $P2_1/n$ |
| a(Å) | 24.100(2) | 11.4258(4) | 15.3368(6) | 18.1374(12) |
| b(Å) | 7.9528(5) | 19.3036(8) | 12.2990(5) | 13.2270(9) |
| c(Å) | 13.4035(11) | 11.4694(4) | 13.0974(6) | 13.2270(9) |
| Volume($Å^3$) | 2547.2(4) | 2415.88(16)) | 2469.76(17) | 18.2619(11) |
| Z | 4 | 4 | 4 | 4 |
| $D_{calcd}$($mg/cm^3$) | 1.578 | 1.667 | 1.469 | 1.568 |
| μ($mm^{-1}$) | 1.357 | 1.446 | 1.392 | 1.619 |
| *F*(000) | 1224.0 | 1208.0 | 1104.0 | 2048.0 |
| θ-range for data collection (°) | 6.618 to 52.038 | 7.338 to 52.04 | 6.94 to 52.04 | 6.562 to 52.044 |
| Reflections collected | 9637 | 10068 | 9299 | 17186 |
| Independent Reflections | 5015 [$R_{int}$=0.0586] | 4620 [$R_{int}$=0.0365] | 4850 [$R_{int}$= 0.0454] | 8582 [$R_{int}$= 0.0484] |
| Data/restraints/ Parameters | 5015/0/344 | 4620/39/361 | 4850/0/300 | 8582/36/569 |
| Final R-indices [$I \geq 2\sigma(I)$] | $R_1$ = 0.0603, $wR_2$ = 0.0822 | $R_1$ = 0.0446, $wR_2$ = 0.0975 | $R_1$ = 0.0546, $wR_2$ = 0.0948 | $R_1$ = 0.0442, $wR_2$ = 0.0845 |
| Final R indices | $R_1$ = 0.1400, | $R_1$ = 0.0742, | $R_1$ = 0.0977, | $R_1$ = 0.0723, |

| | | | | |
|---|---|---|---|---|
| [all data] | $wR_2$ = 0.1093 | $wR_2$ = 0.1166 | $wR_2$ = 0.1152 | $wR_2$ = 0.1000 |
| Largest diff.peak and hole (e Å$^{-3}$) | 0.40/-0.39 | 0.42/-0.33 | 0.45/-0.33 | 0.31/-0.42 |

The ability of CO-release was evaluated in a myoglobin-based aqueous assay. A solution of deoxymyoglobin was prepared and subsequently treated with a solution of the CORM at 37.5 °C. The resulting conversion of deoxy-Mb to CO-Mb was monitored by UV–vis spectroscopy. To evaluate both the total amount of CO released and the rate of CO release, all complexes were tested at 10 μ M by following the changes in absorption. A representative example of the UV spectrum and the concentration of CO-Mb as a function of time are given in Fig. 2 (for other complexes see SI-Fig. 1). The half-lives of all the complexes are listed in Table 2. As seen from the data, the half-lives of complexes **12** and **13** were 25.6 min and 26.8 min respectively, while complex **15** was 15.8min which shows it was a fast CO-releaser. Like the complexes reported before [40], the half-lives were also dependent on the structures of non–CO ligands. For the complexes containing Ar-NH-Ar' structure (complexes **2**, **6**, **7**, **9**, **10**), the $T_{1/2}$ of the complex having pyridine ring was longer than the others, the electron withdrawing group at the m-position of Ar ring ($CF_3$, Cl) made CO releasing slower, for example, the $T_{1/2}$ of complex **6** was up to 42.6min, in contrast, complex **7** containing methyl only 26.4min.

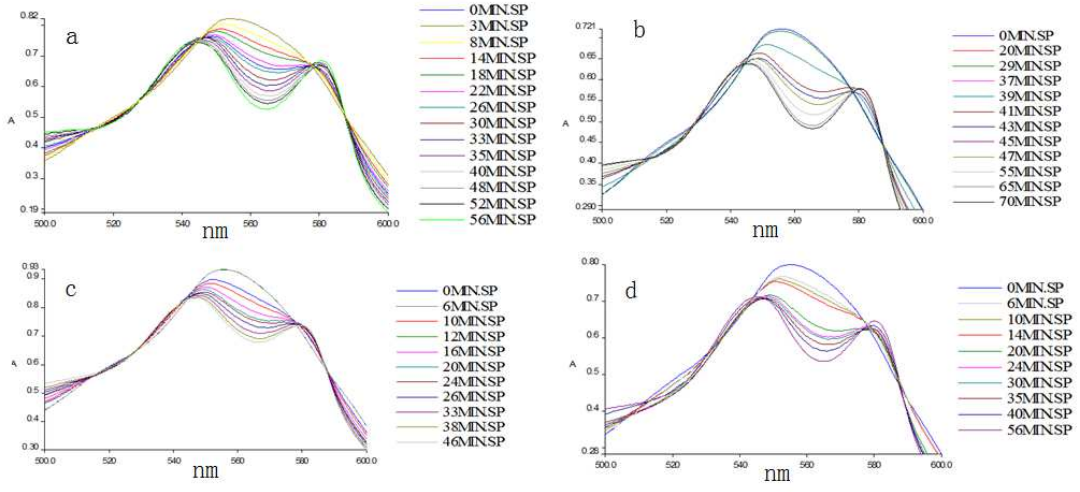


**Fig. 2** The typical changes in the electronic spectrum of myoglobin as CO releasing from compounds (myoglobin binds one CO to form carbonyl myoglobin), A, complex 1 (10 μM); B for 5 (10 μM); C for 10(10 μM); D for 15 (10 μM).

To evaluate the capacity of permeable membrane of complex in vivo, we measured lgP values using n-octanol/water system. Their lgP values were in the range of 1.62 and 2.16. The values of complexes **12** and **13** are 1.91 and 2.03 respectively.

Our previous studies show cobalt complexes were unevenly distributed in tissues and organs; some have a big prone to collect in liver, whereas some easily enter to kidney. The substituents significantly affected the rate of CO-release, cytotoxicity and their bio-distribution.

**Table 2** Physical-chemical parameters of all the complexes.

| Complex | $T_{1/2}$（min） | lgP | Complex | $T_{1/2}$（min） | lgP |
|---|---|---|---|---|---|
| **1** | 32.8 | 2.16 | **9** | 30.9 | 1.85 |
| **2** | 21.8 | 1.98 | **10** | 24.8 | 2.32 |
| **3** | 30.5 | 1.80 | **11** | 16.9 | 2.05 |
| **4** | 34.7 | 1.96 | **12** | 25.6 | 1.91 |
| **5** | 38.9 | 1.89 | **13** | 26.8 | 2.03 |
| **6** | 42.6 | 1.68 | **14** | 16.3 | 2.12 |
| **7** | 26.4 | 2.10 | **15** | 15.8 | 1.62 |
| **8** | 16.8 | 2.06 | | | |

### 2.2 Anti-tumor activities of complex and effect on COX-2 expression level

Growth inhibitory effect toward the cancer cell line was determined by MTT method. As shown in Table 3, all the complexes displayed lower activities than cis-platin on the proliferation of five tumor cells, and most of them had low selectivity to normal cells W138 and tumor cells. But compared with 5-FU, some displayed better activity; among them, complexes **4**, **12** and **13** had higher selectivity to HT-29 cell lines and MCF-7, and selective index was up to 2.94 at most. Complexes **12** and **13** were significantly more effective against proliferation of all five tumor cells than others. For HT-29 cell lines, their $IC_{50}$ values were 37.9μM and 55.8μM respectively, and 33.6μM and 49.3μM respectively for MCF-7 cell lines. Except the structure factor of the side chains, this probably closely connected with celecoxib and nimesulide biological function which were selective COX-2 inhibitors.

**Table 3** $IC_{50}$ values of complex to tumor cells and W138

| Complex | $IC_{50}$(μM) | | | | | |
|---|---|---|---|---|---|---|
| | Hella | A549 | HT-29 | HePG2 | MCF-7 | W138 |
| **1** | 143.6±3.9 | 126.8±3.5 | 95.8±4.8 | 136.8±5.8 | 128.8±5.2 | 168.9±4.7 |
| **2** | 129.6±4.5 | 133.4±5.2 | 83.6±2.1 | 121.8±4.9 | 110.8±2.9 | 146.8±5.1 |
| **3** | 141.8±6.7 | 128.9±3.9 | 108.7±1.8 | 118.8±3.6 | 98.7±6.3 | 139.8±6.1 |
| **4** | 91.8±6.6 | 72.3±4.4 | 65.5±2.4 | 82.6±4.2 | 52.8±3.3 | 109.8±3.6 |
| **5** | 127.7±4.2 | 136.8±5.3 | 98.6±3.7 | 118.7±6.1 | 106.2±4.5 | 130.8±4.6 |
| **6** | 141.6±4.9 | 152.8±6.1 | 132.6±2.1 | 161.8±3.9 | 121.6±4.1 | 132.8±5.1 |
| **7** | 117.6±5.8 | 129.8±3.7 | 109.8±3.4 | 109.6±4.8 | 88.9±2.5 | 168.9±6.8 |
| **8** | 198.8±4.3 | 241±3.6 | 218.9±4.9 | 232.5±6.8 | 178.8±3.9 | 218.9±4.1 |
| **9** | 128.7±5.1 | 165.6±5.2 | 139.8±5.3 | 141.5±4.8 | 108.3±5.7 | 136.8±4.9 |

| | | | | | | |
|---|---|---|---|---|---|---|
| **10** | 132.8±2.9 | 159.3±4.7 | 129.8±3.2 | 109.8±5.1 | 118.6±6.1 | 154.8±6.1 |
| **11** | 108.6±6.1 | 109.3±3.8 | 120.8±1.5 | 136.8±5.4 | 102.8±4,4 | 142.8±4.2 |
| **12** | 77.9±4.6 | 59.8±3.9 | 37.9±3.7 | 60.7±3.9 | 33.6±2.4 | 98.8±6.4 |
| **13** | 71.5±4.8 | 63.8±4.6 | 55.8±5.9 | 69.8±4.9 | 49.3±2.9 | 92.6±4.8 |
| **14** | 189.8±4.9 | 209.8±5.1 | 202.7±4.1 | 241.8±6.3 | 238.7±6.9 | 289.8±3.9 |
| **15** | 129.8±5.7 | 90.5±3.6 | 89.6±3.1 | 89.9±5.2 | 72.8±4.1 | 169.8±5.4 |
| **16** | 86.8±5.4 | 92.8±5.7 | 73.2±5.6 | 66.8±6.1 | 66.8±3.6 | 82.5±3.9 |
| **5-FU** | 114.2±4.9 | 98.7±4.2 | 136.2±3.9 | 124.3±10.3 | 148.7±5.2 | 198.6±3.6 |
| **DDP** | 34.7±3.2 | 29.6±1.9 | 30.6±1.2 | 24.6±2.2 | 25.5±1.8 | 50.3±4.2 |

In order to confirm the important role of COX-2 in anti-proliferation, we measured the survival rates of HT-29 and MCF-7 cells after treated with precursors and complexes respectively. Seen from Fig.2-SI, in the range of 6.5-800μM, all compounds showed better activities against tumor cells, and the survival rates of HT-29 and MCF-7 cells decreased with the increase of the concentration, this indicates COX-2 was one of targets of the complex; moreover, complexes **4**, **12** and **13** had higher inhibitory rates of proliferation than the corresponding precursors, $A_4$, $A_{12}$ and $A_{13}$, which indicates the complexes may be multi-target anticancer agents. In contrast, the activities of complexes **12** and **13** were higher than that of **4**, this is because $A_{12}$ and $A_{13}$ were selective COX-2 inhibitors and $A_4$ was non-selective COX-2 inhibitors. This suggests down-regulation of COX-2 level should inhibit the proliferation of tumor cells.

To figure out the relationship between the up-regulation or down-regulation of COX-2 expression and the anti-tumor activity of the complex, the effect of concentration on the expression level of COX-2 in HT-29 cells and MCF-7 cells was further investigated.

The results showed that all the tested compounds inhibited the expression of COX-2 in HT-29 cells, and complexes **4**, **12** and **13** had stronger inhibitory effects on COX-2 than the corresponding $A_4$, $A_{12}$ and $A_{13}$. Seen from Fig.3, complex **4** displayed lower activity to inhibit COX-2 expression level at 10uM, but when it was over 50uM, its activity was very significant. Complex **12** distinctly inhibited the expression of COX-2 at 10μM, and the down-regulation trend was obvious in a dose-dependent manner. Complex **13** was similar to **12**, but its activity was slightly lower than that of **12**. This indicates that the stronger the complex inhibiting COX-2 expression, the higher the activity of the complex. This was consistent with the conclusion that the cell survival rate was lower.

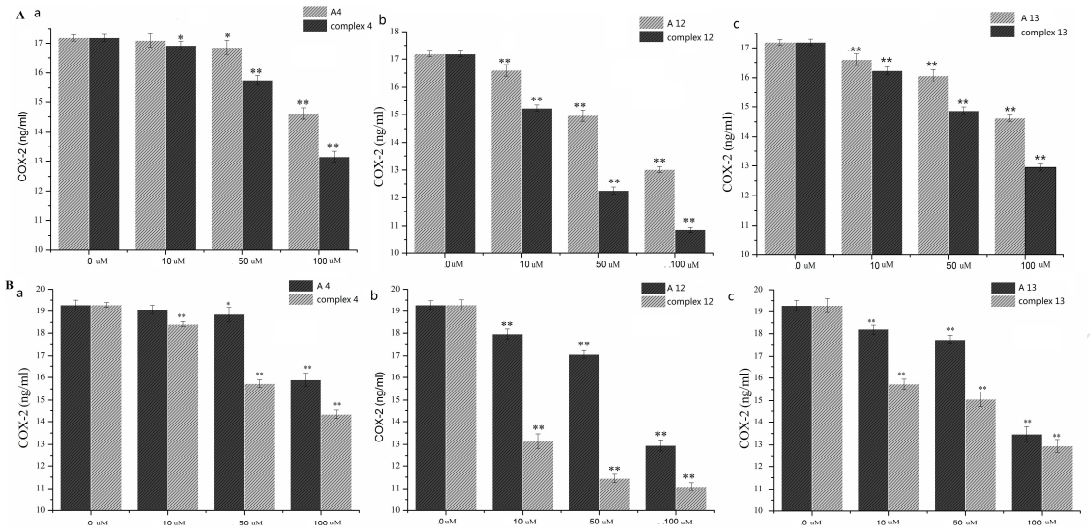


Fig. **3** The effect of compound concentration on COX-2 in HT-29(A) and MCF-7 cells; (B): a for complex **4** and $A_4$, b for complex **12** and $A_{12}$, c for complex **13** and $A_{13}$

For MCF-7 cell lines, all the tested compounds also inhibited the expression of COX-2 (Fig. 3), and the inhibitory trend with the concentration was similar to HT-29 cells. Distinctly, these compounds inhibited COX-2 level expression in MCF-7 more strongerly than in HT-29 cells, especially for complex **12**.

**2.3 Protective effect of complex on oxidative damage of rat myocardial H9c2 cells**

Celecoxib was selective COX-2 inhibitors which used clinically as NSAIDs, but it withdrew from market due to myocardiotoxicity. CORMs had protective effect on myocardial ischemia-reperfusion injury. [41] Modified with CORMs, they will possibly improve these side-effects by CO biological function. In order to verify validation of this idea, we chose H9C2 cells treated with $H_2O_2$ as an in vitro model of myocardial ischemia-reperfusion injury.

To obtain more accurate information about myocardial cell protection, the toxicities of the tested complexes to H9c2 cells were evaluated at first. The cell survival rates were greater than 90% after the H9c2 cells treated with the complex at the set concentration range, which indicates the set concentration was effective and rational in the protective effect of H9c2 cells. And the cell survival rate was 80.46%, 70.96% and 64.28%, respectively, after treatment with 400μM $H_2O_2$ for 1h, 4h and 8h.

Then, the cells were treated with 400μM $H_2O_2$ for 1h (or 4h, or 8h), and incubated with complex (**1**, or **10** or **12**) at different concentrations (10μM, 25μM and 50μM) the repair effects on H9c2 were detected.

The results showed all three complexes improved the survival rate of H9c2 cells injured by $H_2O_2$ (Fig.4). The survival rate increased most obviously after the cells

treated with $H_2O_2$ for 1h for each tested complex, and it increased least when the cells harmed for 8h due to the severe cell injury. H9c2 cells treated for 1h, complex **1** increased the survival rate of 13.35%, and for 8h, it increased below 10% (Fig.4); for complex **12**, the survival rate of H9c2 cells was only increased by 3.55% after $H_2O_2$ injury for 8h (Fig.4). As a whole, after 1h of injury, complex **1** had the strongest ability to improve H9c2 cell viability, and complex **12** distinctly improved the cell survival rate; and for each tested complex, the increasing survival rate of H9c2 cells was not in a dose-dependent manner. When the tested complex was 50μM, they had a maximal efficacy to repair damaged H9c2 cells.

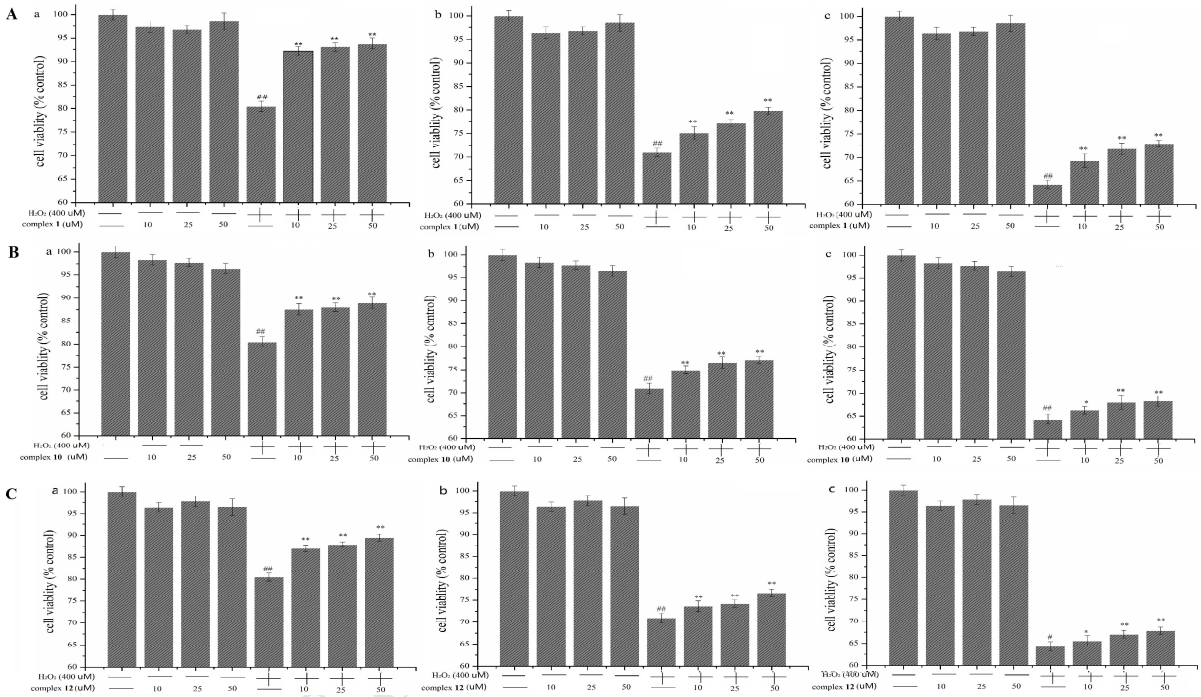


Fig. **4** Effect of complex **1**, **10** and **12** on the viability rate of H9c2 cell treated with $H_2O_2$ for different time: a for 1h, b for 4h, c for 8h. Each experimental concentration set 6 sets of parallel experiments, expressed by mean ±SD; * represents testing group and $H_2O_2$ group $P < 0.05$; ** represents testing group and $H_2O_2$ group $P < 0.01$; # represents compared with the blank control ($p < 0.01$).

After H9c2 cells were damaged by $H_2O_2$, the CO released by the complexes increased the survival rate of H9c2 cells, and displayed a protection against H9c2 cells injury. To preliminary understand the mechanism of action, the level of SOD and MDA in H9c2 cells was measured. The results showed, after H9c2 cells treated with $H_2O_2$ for 1h the content of SOD decreased, but it increased significantly after administration of complex **12**; Moreover, with the concentration of the complex **12**

increasing, the content of SOD increased (Fig.5). At the same time, the level of MDA decreased significantly with the complex increasing (Fig.5). In contrast, the activity of complex **12** was as strong as that of complex **10**, and complex **1** was stronger than those of complexes **10** and **12**. All that suggests the complexes protected H9C2 cells from antioxidant damage by the way which increase SOD level and low MDA level.

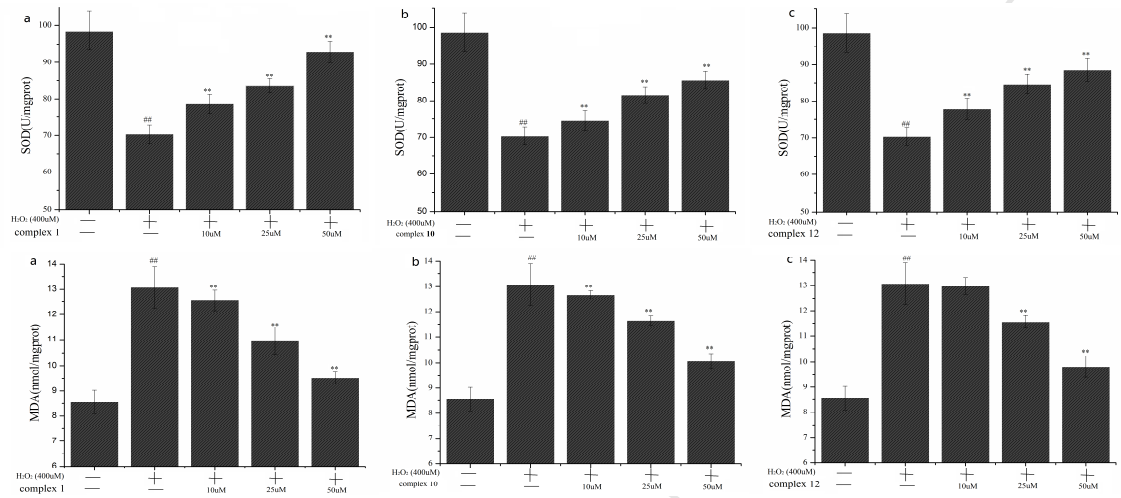


**Fig. 5** Effect of complex on SOD and MDA content of H9C2 cells treated with $H_2O_2$ for 1h. Six groups of parallel experiments were set up in each content, and the data were expressed as mean ±SD. ** represents $P < 0.01$ for testing group and $H_2O_2$ group; $^{\#\#}$ represents $P < 0.01$ for testing group and blank group

## 2.4 Antihypertensive effect of target complex in SHR

It has been shown that CO relaxed the blood vessels and protected the heart, which was related to the activity of CO regulating the activity of vascular endothelial factor. [42] CO acted on the peripheral blood vessels and maybe participated in the regulation of blood pressure. To prove this idea, we selected the spontaneously hypertensive rats SHR, evaluated the antihypertensive effect of the complex. The results showed that all the tested complexes had antihypertensive effect on SHR rats. As shown in Fig. 6, complex **1** which modified by indomethacin decreased the systolic blood pressure of SHR rats compared with the control group (165mmhg); When the concentration was 10, 20 and 40 mg/kg, the blood pressure of SHR dropped to 154.7, 142.6 and 134.6 mmHg; for complex **10** which modified by diclofenac, after administration of 10, 20 and 40 mg/kg, the contraction pressure of SHR rats decreased to 147.6, 144.5 and 135.8mmHg. Compared with the control group (165mmhg), complex **1** almost had the same antihypertensive effect as complex **10**. But for complex **12**, it showed stronger activity than those in the same condition, the systolic

blood pressure of SHR rats were decreased to 135.7, 128.7 and 117.5mmHg. This effect was also concentration dependent. Meanwhile, the tested complexes also reduced the diastolic blood pressure, and the trend was consistent with the decrease of the systolic blood pressure (see in Fig.**6**). Though the antihypertensive effect of complex originated from CO released from it, the structure of NSAIDs had remarkable effect on anti-hypertension, just like the effect of substituent on CO release rate.

However, compared with nifedipine and captopril, the antihypertensive effects of the complexes were less at the same concentration. It showed that the regulating effect of the complexes on blood pressure was limited.

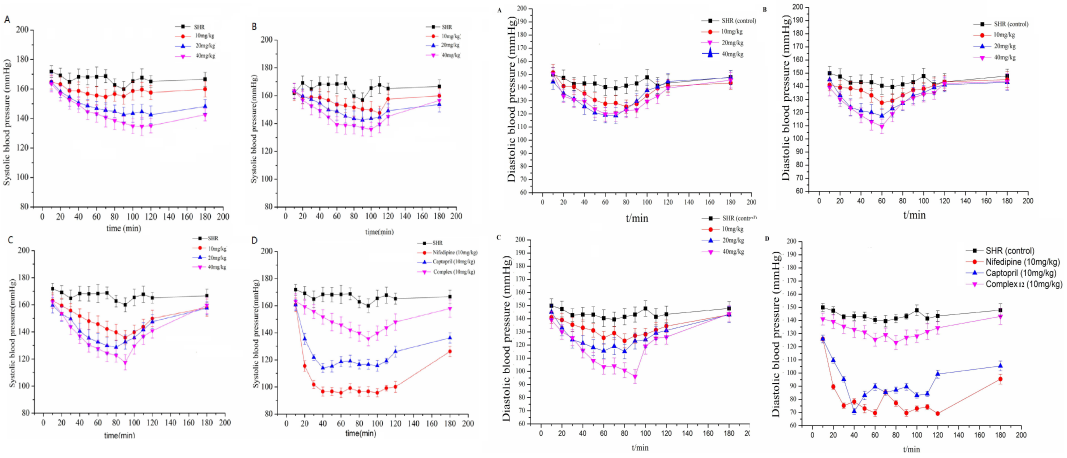


**Fig**. **6** Effect of the complex on systolic blood pressure and diastolic blood pressure in SHR, A for complex **1**, B for **10**, C for **12**; D, the anti-hypertension effects of complex **12**, captopril and nifedipine at 10mg/kg

## 2.5 Myocardial protective effects of complex for SHR

In the process of studying anti-hypertension of the complex, considering the protection of complex against H9c2 cell injury, we wonder whether the complex is effective to animal model. By the way, we used optical microscope and TEM to observe the change of myocardial structure after administrating tested complexes 14 days.

We found that the control (celecoxib) group, myocardial fibers arranged neatly in SHR, muscle clearance was increased in different degree, and collagen fibers were found in some of the interstitium. But for the myocardial structures in SHR treated with complex **1** or **12**, myocardial fibers arranged neatly, occasionally found boudoir disc; the nucleus was located in the center of the muscle fibers, and muscle gap slightly increased, no obvious interstitial collagen fiber was found. Through TEM, we can see in Fig.7, in control group, myocardial interstitial vascular swelling, loose

arrangement of muscle fibers, muscle fiber membrane swelling, myocardial fiber melting, contraction band formation, myocardial intercalated discs dissociation and swelling of mitochondria. But in contrast, for complex **1** or **12** group, myofibril basic was basically regular and no obvious lysis of myofilament; mitochondrial swelling was not significant and no myocardial intercalated discs dissociation were found.

Distinctly, the complexes protected the myocardium in some degree caused by celecoxib. We know celecoxib is a selective inhibitor of COX-2, and its toxic effects for heart and blood vessels may result from inhibiting the COX-2 activities at the special organs and tissues, because many testing results proved COX-2 mediated delayed myocardial protection. Therefore, we conclude that this myocardial protective effect was mediated by CO released from the tested complex.

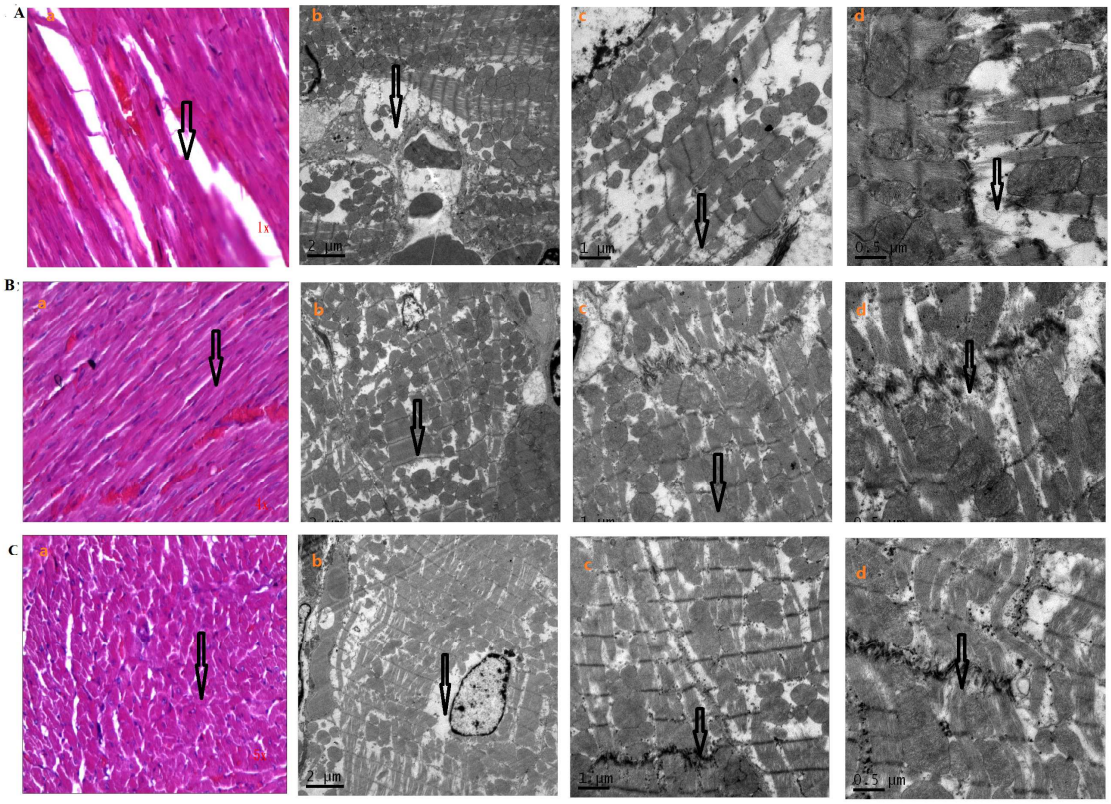


**Fig. 7** Optical microscopy (color) and TEM morphological images of cardiac muscle cell from tested SHR: Myocardial protective effect of the complex appeared after administrating a certain dose tested complex successively 14 days. The morphological cells are seen in different states：A for celecoxib，B for complex **1**，C for complex **12**. The arrows in A(a), B(a) and C(a) (6,000-fold) indicate myocardial fiber bundles gap; The arrows in A(b), B(b) and C(b) (10,000-fold) indicate the swelling of myocardial fibers; A(c), B(c) and C(c) (210,000-fold) indicates dissolution of the myocardial fibers; A(d), B(d) and C(d) (20,000-fold) arrows indicate myocardial intercalated discs.

## 2.6 Liver and kidney toxicity of complex for SHR

Similarly, through optical microscope (Fig.8), for the SHR treated with complex **1** or **12**, we saw the hepatic lobule was complete; congestion of central venous and congestion of hepatic sinusoid were obvious; liver cell was swelling and cytoplasm staining was pale. Meanwhile, the the renal glomerulus was intact; the proximal tubule cells were swelled, the cytoplasm was loose and pale, and some renal tubular epithelial cells were necrotic. Under TEM, we found liver cell nucleus abnormal, heterochromatin increase, chromatin margination, lipid droplets increase in the cytoplasm and hepatic blood sinus Dirichlet space widened.

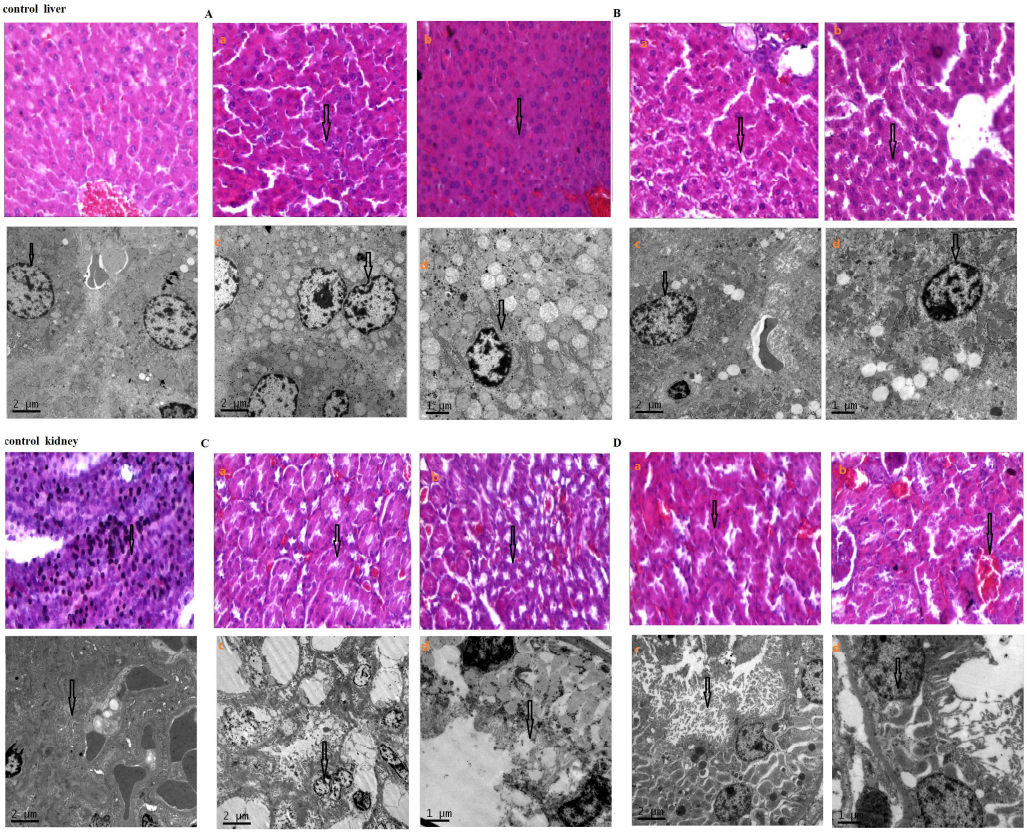


**Fig. 8** Optical microscopy (color) and TEM morphological images of liver and kidney cells from tested SHR after administrating a certain dose complex successively 14 days: A for and B, the morphological liver cells treated with complex **1** and complex **12**. C and D, the morphological kidney cells treated with complex **1** and complex **12** respectively. The arrows in A(c, d) and B(c, d) arrows indicate abnormal nuclear morphology; the arrows in C(c, d) indicate swelling of glomerular endothelial cells, a large amount of exudation in glomeruli; D(c, d) indicate mesangial cell proliferation, irregular proximal convoluted tubule villus.

Meanwhile, the glomerular endothelial cells were swelling with stromal hyperplasia and exudation in the glomerulus; the proximal tubule microvilli exfoliated loosed and the foot processes were fusion. In contrast, the side-effect on kidney

caused by complex **12** was more serious. This demonstrates the two complexes which administrated continuously are still not safe for 14 days.

## 3. Conclusion

Carbon monoxide (CO) is an important signaling molecule as NO. CORMs are hoped to deliver controlled amounts of CO directly to tissues or organs. CORMs containing cobalt are complex. Most of them inhibited tumor cell proliferation, and their activities were connected with the structures of non-CO ligands. Based on COX-2 role in tumorigenesis, development and metastasis of cancer, we synthesized hybrid CORMs containing NSAIDs structure. Compared with cisplatin, all the complexes displayed low activities against proliferation of five kinds of tumor cells. But complexes **12** and **13** displayed better activities and selectivity to HT-29 and MCF-7 cell lines compared with 5-FU. In contrast, complexes **12** and **13** were more effective against tumor cells; moreover, complex **12** was stronger to down-regulate COX-2 expression level than complex **4**. Possibly, this is because complex **12** contained celecoxib structure fragment, which was a COX-2 selective inhibitor. We found the complex inhibited the expression of COX-2 in HT-29 cells and MCF-7cells, in accordance with its activity against tumor cell proliferation. Of course, seen from the $IC_{50}$ values of all the complexes, their activities were not very high. However, this does not stand for these complexes have no value to further investigate, because whether they inhibitor tumor cell metastasis and tumorigenesis, it needs us to further investigate. As expected, the complex increased the survival rate of myocardial H9c2 cells after the cells treated with $H_2O_2$, which indicates the complexes have protective effect on oxidative damage of rat myocardial H9c2 cells. But this protective effect was not obvious when the cells harmed for 8h due to the severe cell injury. In addition, the compound had concentration dependent antihypertensive effect on SHR rats, accompanying with good myocardium protection. This indicates these hybrid CORMs reduced side-effects of COX-2 inhibitors, but there still have liver and kidney side-effects when administrating continuously for 14 days.

## 4. Experimental

### 4.1 Reagents and instruments

Myoglobin (AR, Sigma), BCA protein quantification kit (Sigma), ELISA kit (Sigma). Captopril and nifedipine nifelat (AR) were purchased from Beijing bailingwei Technology Co. Hela cell ,HepG2 cell ,MCF-7 cell ,A549 cell ,HT-29 cell and W138 cell lines were purchased from the cell resources Center for Shanghai Life Science Institute of Chinese Academy of Sciences (China). Clean grade male spontaneously hypertensive rats (SHR) rats and WKY (Wistar-Kyoto) rats were provided from the Animal Center of GLP, Lanzhou University. Laboratory animal qualification: SCXK (GAN) 2009-2004. Rats were fed in cage, kept at

room temperature (23±2)□, relative humidity 60-65%, free eating and drinking water.

Blood press was measured using BP-300A Automatic non-invasive blood pressure detector (Chengdu, taimeng, China, Software Co. Ltd.).

All reactions were carried under nitrogen atmosphere. Solvents for reactions were degassed and distilled from the proper drying agents. Column chromatography was carried out using 200-300 mesh silica gel.

IR spectra were recorded on a Nicolet NEXUS 360 spectrophotometer, and NMR spectra on a BrukerAM-400 MHz spectrometer. A Lambda 25 UV-Visible spectrophotometer and a Maxis-4G TOF Mass spectrometer (ESI) were used.

**4.2 Synthesis of the complexes**

The preparation of compound **$A_1$**

To the solution of (indomethacin, 357 mg 1.0mmol) in 8mL of acetonitrile, DMAP (18mg, 0.15mmol) and EDCI (190mg, 1.0mmol) were added with stirring at room temperature for 0.5h. Then, propargyl alcohol (0.07ml, 1.0mmol) was added to the mixture solution and stirred for 4h. After filtration, the filtrate was evaporated under reduced pressure to remove the solvent. The oily residue was dissolved in trichloromethane; the organic layer was washed with brine and dried with anhydrous $Na_2SO_4$, then filtered; the solvent was removed. The crude product was chromatographed on a silica gel, and 260 mg white solid was obtained. Yield: 65.8%. Ethyl acetate/hexane (1:15); $R_f$ =0.28. $^1$H NMR ($CDCl_3$) δ 7.60 (dd, *J* = 8.7, 2.0 Hz, 2H), 7.43 – 7.38 (m, 2H), 6.89 (d, *J* = 2.4 Hz, 1H), 6.80 (d, *J* = 9.0 Hz, 1H), 6.60 (dd, *J* = 9.0, 2.4 Hz, 1H), 4.64 (d, *J* = 2.4 Hz, 2H), 3.77 (s, 3H), 3.65 (s, 2H), 2.41 (t, *J* = 2.4 Hz, 1H), 2.32 (s, 3H). ESI-HRMS (m/z): calcd for $C_{23}H_{18}ClNNaO_4$ $[M+Na]^+$ 418.0822,found 418.0814.

The preparation of compound **$A_2$-$A_{11}$**

The preparation and workup of compounds **$A_2$-$A_{11}$** were similar to **$A_1$**. Compound **A2:** white solid 168 mg. Yield: 60.2%. Ethyl acetate/hexane (1:10); $R_f$ = 0.32. $^1$H NMR ($CDCl_3$) δ 9.07 (s, 1H), 7.93 (dd, *J* = 8.0, 1.6 Hz, 1H), 7.18 (s, 1H), 7.05 (dt, *J* = 15.0, 7.8 Hz, 2H), 6.96 (d, *J* = 7.2 Hz, 1H), 6.66 (d, *J* = 8.6 Hz, 1H), 6.60 (t, *J* = 7.8 Hz, 1H), 4.85 (d, *J* = 2.5 Hz, 2H), 2.45 (t, *J* = 2.5 Hz, 1H), 2.26 (s, 3H), 2.10 (s, 3H). ESI-HRMS (m/z): calcd. for $C_{18}H_{18}NO_2$ $[M+H]^+$: 280.1338. found 280.1338; calcd. for $C_{18}H_{17}NNaO_2$ $[M+Na]^+$: 302.1157; found 302.1173.

Compound **$A_3$:** yellow Oil. Yield: 56.2%. Ethyl acetate/hexane (1:10); $R_f$ =0.32. $^1$H NMR ($CDCl_3$) δ 7.77 – 7.70 (m, 2H), 7.68 (t, *J* = 1.6 Hz, 1H), 7.61 (dt, *J* = 8.0, 1.6 Hz, 1H), 7.49 (ddt, *J* = 14.8, 7.7, 1.8 Hz, 2H), 7.40 (dd, *J* = 15.2, 7.8 Hz, 3H), 4.60 (qd, *J* = 15.6, 2.4 Hz, 2H), 3.77 (q, *J* = 7.2 Hz, 1H), 2.37 (t, *J* = 2.4 Hz, 1H), 1.48 (d, *J* = 7.0 Hz, 3H). ES I-HRMS (m/z): calcd. for $C_{19}H_{16}NaO_3$ $[M+Na]^+$: 345.0997; found 315.0986.

Compound **$A_4$:** pale yellow solid 288.8mg; Yield: 73.1%. Ethyl acetate/hexane (1:20);Rf=0.43. $^1$H NMR (400 MHz, Chloroform-*d*) δ 7.76 – 7.51 (m, 4H), 7.17 (s, 1H), 7.10 (s, 1H), 6.81 (dd, *J* = 8.9, 2.4 Hz, 1H), 6.50 (td, *J* = 8.8, 2.5 Hz, 1H), 4.64 (d, *J* = 2.5 Hz, 2H), 3.55 (s, 2H), 2.74 (s, 3H), 2.42 (t, *J* = 2.5 Hz, 1H), 2.14 (s, 3H). ESI-HRMS (m/z): calcd. for $C_{22}H_{20}FO_3S$ $[M+H]^+$: 395.1117; found 395.1125, $C_{22}H_{20}FO_3SNa$ $[M+Na]^+$: 417.0937; found 417.0945.

Compound **$A_5$:** white solid 138.2 mg; Yield: 48.94%. Ethyl acetate/hexane (1:4);Rf=0.28.$^1$H NMR ($CDCl_3$) δ 7.46 (dt, *J* = 8.0, 1.6 Hz, 2H), 7.39 – 7.33 (m, 2H), 7.32 – 7.27 (m, 2H), 7.10 – 7.03 (m, 2H), 4.70 – 4.53 (m, 2H), 3.73 (q, *J* = 7.2 Hz, 1H), 2.39 (t, *J* = 2.4 Hz, 1H), 1.48 (d, *J* = 7.2 Hz, 3H). ESI-HRMS (m/z): calcd. for $C_{18}H_{15}FNaO_2$ $[M+Na]^+$: 305. 0954; found 305.0944.

Compound **$A_6$:** white solid 126.9mg； Yield: 42.30%. Ethyl acetate/hexane (1:10);Rf=0.36$^1$H NMR (400 MHz, Chloroform-*d*) δ 9.74 (s, 1H), 8.37 – 8.13 (m, 2H), 7.77 (dd, *J* = 7.5, 2.0 Hz, 1H), 7.12 – 7.07 (m, 2H), 6.67 (dd, *J* = 7.8, 4.7 Hz, 1H), 4.88 (d, *J*=2.5Hz,2H), 2.49(t, *J*=2.4Hz, 1H), 2.32(s,3H). ESI-HRMS(m/z): calcd.for $C_{16}H_{14}ClN_2O_2[M+H]^+$:301.0744;found301.0740,$C_{16}H_{13}ClN_2NaO_2[M+Na]^+$: 323.0563; found 323.0560.

Compound **$A_7$:** white solid 150.2mg； Yield: 46.93%. Ethyl acetate/hexane (1:6); $R_f$=0.30.$^1$H NMR ($CDCl_3$) δ 9.43 (s, 1H), 7.96 (dd, *J* = 8.1, 1.7 Hz, 1H), 7.41 (s, 1H), 7.38 – 7.28 (m, 3H), 7.24 (d, *J* = 7.3 Hz, 1H), 7.22 – 7.17 (m, 1H), 6.84 – 6.61 (m,1H),4.84(d,*J*=2.5Hz,2H),2.46(t,*J*=2.5Hz,1H).ESI-HRMS(m/z):calcd.for$C_{17}H_{13}F_3NO_2[M+H]^+$:320.0986;found320.0999.

Compound **$A_8$:** white solid 120.6 mg； Yield: 42.17%. Ethyl acetate/hexane (1:10);Rf=0.32.$^1$H NMR ($CDCl_3$) δ 8.42 (s, 1H), 8.09 (dt, *J* = 7.8, 1.6 Hz, 1H), 7.96 – 7.91 (m, 1H), 7.40 (d, *J* = 7.6 Hz, 1H), 4.86 (d, *J* = 2.4 Hz, 2H), 2.44 (t, *J* = 2.4 Hz, 1H), 1.29 (s, 12H). ESI-HRMS (m/z): calcd. for $C_{16}H_{19}BNaO4$ $[M+Na]^+$: 309.1274; found 309.1265.

Compound **$A_9$:** white solid 120.6 mg； Yield: 42.17%. Ethyl acetate/hexane (1:3);Rf=0.36.$^1$H NMR ($CDCl_3$) δ 10.18 (s, 1H), 8.58 – 8.19 (m, 2H), 8.01 (s, 1H), 7.81 (s, 1H), 7.38 (t, *J* = 7.8 Hz, 1H), 7.24 (s, 1H), 6.76 (d, *J* = 4.6 Hz, 1H), 4.88 (d, *J* = 2.4 Hz, 2H), 2.50 (t, *J* = 2.4 Hz, 1H). ESI-HRMS (m/z): calcd. For$C_{16}H_{12}F_3N_2O_2$ [M+H]+: 321.0861， found 321.0891.

Compound **$A_{10}$:** white solid 136.6 mg. Yield: 40.8%. Ethyl acetate/hexane (1:5);Rf=0.43.$^1$H NMR ($CDCl_3$) δ 7.27 (d, *J* = 8.0 Hz, 2H), 7.19 (d, *J* = 2.8 Hz, 1H), 7.07 (td, *J* = 7.6, 1.6 Hz, 1H), 6.94 – 6.87 (m, 2H), 6.49 (dd, *J* = 8.0, 1.2 Hz, 1H), 4.68 (d,*J*=2.5Hz,2H),3.80(s,2H),3.42(s,1H),2.42(t,*J*=2.5Hz,1H).ESI-HRMS(m/z):calcd.For$C_{17}H_{14}Cl_2NO_2[M+H]^+$:334.0462;found334.0475.

Compound **$A_{11}$:** white solid 112.4 mg. Yield: 35.3%. Ethyl acetate/hexane (1:2); Rf=0.31. $^1$H NMR ($CDCl_3$) δ 7.83 (d, *J* = 7.6 Hz, 1H), 7.75 (d, *J* = 8.2 Hz, 2H), 7.51

(t, *J* = 7.4 Hz, 1H), 7.43 (d, *J* = 8.0 Hz, 2H), 7.30 (s, 2H), 4.77 (s, 2H), 4.68 – 4.49 (m, 2H), 3.70 (q, *J* = 7.2 Hz, 1H), 2.38 (t, *J* = 2.5 Hz, 1H), 1.45 (d, *J* = 7.2 Hz, 3H). ESI-HRMS (m/z): $C_{20}H_{17}NNaO_3$ $[M+Na]^+$: 342.1156; found 342.1177.

The preparation of compound **$A_{12}$-$A_{13}$**

Compound **$A_{12}$:** To the solution of (celecoxib, 1013 mg 3.0mmol) in 20mL of acetone, anhydrous potassium carbonate (167 mg, 1.2mmol) were added with stirring at room temperature for 0.5h. Then 3-bromopropyne (0.08 ml, 1.0mmol) was added and stirred for 24h at room temperature. After filtration, the filtrate was evaporated under reduced pressure to remove the solvent. The crude product was chromatographed on a silica gel (ethyl acetate: petroleum ether10:1→3:1), and 298.0 mg white solid was obtained. Yield:23.8 %.$^1$H NMR (400 MHz, Chloroform-*d*) δ 7.81 (d, *J* = 8.7 Hz, 2H), 7.41 (dd, *J* = 8.9, 2.2 Hz, 2H), 7.19 (s, 1H), 7.11 (s, 2H), 7.03 (d, *J* = 8.2 Hz, 2H), 6.67 (s, 1H), 3.80 (dd, *J* = 6.1, 2.6 Hz, 2H), 2.31 (s, 3H), 2.02 (t, *J* = 2.5 Hz, 1H).ESI-HRMS (m/z): calcd. for $C_{20}H_{16}F_3N_3NaO_2S$ $[M+Na]^+$:442.0813; found 442.0820.

Compound **$A_{13}$:** To the solution of (nimesulide, 308 mg 1.0mmol) in 10mL of acetone, anhydrous potassium carbonate (167mg, 1.2mmol) were added with stirring at room temperature for 0.5h. To the reaction 3-bromopropyne (0.08ml, 1.0mmol) was added and stirred for 24h at room temperature. After filtration, the filtrate was evaporated under reduced pressure to remove the solvent. The crude product was chromatographed on a silica gel (thyl acetate: petroleum ether 5:1, Ethyl acetate/hexane (1:5);Rf=0.35), and 280.0 mg white solid was obtained. Yield: 80.6 %. $^1$H NMR (400 MHz, DMSO-$d_6$) δ 8.02 (dd, *J* = 8.7, 2.6 Hz, 1H), 7.82 (d, *J* = 8.7 Hz, 1H), 7.56 – 7.50 (m, 2H), 7.48 (d, *J* = 2.6 Hz, 1H), 7.33 (s, 1H), 7.28 – 7.24 (m, 2H), 4.58 (d, *J* = 2.5 Hz, 2H), 3.39 (t, *J* = 2.4 Hz, 1H), 3.24 (s, 3H).ESI-HRMS (m/z): calcd. for $C_{16}H_{15}N_2O_5S$ $[M+H]^+$: 347.0702; found 347.0727, $C_{16}H_{14}N_2NaO_5S$ $[M+Na]^+$: 369.0521; found 369.0544.

The preparation of compound **$A_{14}$**

To the solution of (ferulic acid ethyl ester 223 mg 1.0mmol) in 10mL of DMF, anhydrous potassium carbonate (207mg, 1.5mmol) were added with stirring at room temperature for 0.5h. Then 3-bromopropyne (0.08ml, 1.0mmol) was added and stirred for 24h at room temperature. After filtration, the filtrate was evaporated under reduced pressure to remove the solvent. The crude product was chromatographed on a silica gel (thyl acetate: petroleum ether 5:1 Ethyl acetate/hexane (1:5); Rf=0.36). And white powder 114 mg was obtained; Yield: 43.6%,$^1$H NMR (400 MHz, Chloroform-*d*) δ 7.56 (d, *J* = 15.8 Hz, 1H), 7.05 – 6.94 (m, 3H), 6.26 (d, *J* = 15.9 Hz, 1H), 4.73 (d, *J* = 2.4 Hz, 2H), 4.19 (q, *J* = 7.1 Hz, 2H), 3.84 (s, 3H), 2.47 (t, *J* = 2.3 Hz, 1H), 1.27 (t, *J* = 7.1 Hz, 3H). ESI-HRMS (m/z): calcd. For $C_{15}H_{17}O_4[M+H]^+$: 261.1127; found 261.1115, $C_{15}H_{16}NaO_4$ $[M+Na]^+$: 283.0946; found 280.0934.

The preparation of compound **$A_{15}$**

To 0.51 g (1.32 mmol) Celecoxib, 0.42 g (2.65 mmol) potassium permanganate in 10 mL water 0.52 mL 2M sodium hydroxide were added and heated to reflux for 6 h. The cooled, brown suspension was filtrated and washed with water. The filtrate was acidified with 2M hydrochloric acid and the white voluminous preticipate was collected and dried in vacuum affording 0.36 g (66%) carboxylic acid **$B_{15}$**.$^1$H NMR (400 MHz, Chloroform-*d*) δ 8.05 – 7.97 (m, 2H), 7.85 (d, *J* = 8.2 Hz, 2H), 7.37 (d, *J* = 8.1 Hz, 2H), 7.26 (d, *J* = 8.0 Hz, 2H), 6.79 (s, 1H), 4.94 – 4.74 (m, 2H), 2.46 (t, *J* = 2.3 Hz, 1H). ESI-HRMS (m/z): calcd. for $C_{17}H_{13}F_3N_3O_4S$ $[M+H]^+$: 412.0579; found 412.0658, $C_{17}H_{12}F_3N_3KO_4S$ $[M+Na]^+$: 450.0138; found 450.0138. To the solution of **$B_{15}$**, 411.80mg 1.0mmol) in 20mL of DMF, DMAP (18mg, 0.15mmol) and EDCI (190mg, 1.0mmol) were added with stirring at room temperature for 0.5h. To the reaction propargyl alcohol (0.07ml, 1.0mmol) was added and stirred for 4h at room temperature. After filtration, the filtrate was evaporated under reduced pressure to remove the solvent. The oily residue thus obtained was dissolved in trichloromethane; the organic layer was washed with brine, with NaCl 5%, and then dried on anhydrous $Na_2SO_4$, filtered and the solvent evaporated. The crude product was chromatographed on a silica gel, and 220.6 mg white solid was obtained. Yield: 49.1%. Ethyl acetate/hexane (1:3); Rf=0.32. $^1$H NMR (400 MHz, Chloroform-*d*) δ 8.01 (d, *J* = 8.2 Hz, 2H), 7.87 (d, *J* = 8.6 Hz, 2H), 7.39 (d, *J* = 8.5 Hz, 2H), 7.27 (d, *J* = 8.2 Hz, 2H), 7.19 (s, 2H), 6.79 (s, 1H), 4.87 (d, *J* = 2.4 Hz, 2H), 2.47 (t, *J* = 2.4 Hz, 1H). ESI-HRMS (m/z): calcd. for $C_{20}H_{14}F_3N_3O_4S$ $[M+H]^+$: 450.0735; found 450.0748.

2. The preparation of complexes **1-15**

The preparation of complex **1:** 395 mg (1.0 mmol) of compound $A_1$ was dissolved in 20 mL of dry THF, and then 456 mg (1.2 mmol) of dicobaltoctacarbonyl was added. The reaction mixture was stirred for 12 h at room temperature. The solvent was removed in vacuo, the residue was extracted by a small amount of $CH_2Cl_2$, and the extract was subjected to silica gel column chromatography. Ethyl acetate/hexane (1:5) eluted the main red band, from which 410 mg (60.29%) of complex **1** as a brown-red oil was obtained.IR (KBr disk, $cm^{-1}$): 2100vs, 2063vs, 2059vs, 2033vs (Co-CO), 1762s, (COO). $^1$H NMR (400 MHz, Chloroform-*d*) δ 7.59 (d, *J* = 8.0 Hz, 2H), 7.40 (d, *J* = 8.1 Hz, 2H), 6.89 (s, 1H), 6.79 (d, *J* = 9.0 Hz, 1H), 6.60 (d, *J* =9.0Hz,1H),5.99(s,1H),5.26(s,2H),3.76(s,3H),3.69(s,2H),2.31(s,3H).$^{13}$CNMR(101M Hz,CDCl3)δ198.1,169.5167,3,155.1,138.2,135.2,132.9,130.2,129.8,129.6,128.1,113.9 ,111.0,110.7,100.2,87.5,70.9,64.4,54.6,28.9,12.3.ESI-HRMS(m/z):calcd.for$C_{28}H_{18}Cl$ $Co_2NO_{10}Na[M+Na]^+$:703.9181; found 703.9175.

The procedure and workup of complexes **2-15** are similar to the process of complex **1**.

Complex **2**: 298.2mg was obtained as red powder. Yield: 52.8%. Ethyl acetate/hexane (1:5);Rf=0.43.IR (KBr disk, $cm^{-1}$): 2099vs, 2053vs, 2031vs, 2007vs (Co-CO), 1686s, (COO). $^{1}$H NMR (400 MHz, Chloroform-*d*) δ 9.21 (s, 1H), 8.00 – 7.95 (m, 1H), 7.21 – 7.15 (m, 1H), 7.05 (dd, *J* = 15.3, 8.0 Hz, 2H), 6.96 (d, *J* = 7.3 Hz, 1H),6.66(d,*J*=8.5Hz,1H),6.58(t,*J*=7.6Hz,1H),6.06(s,1H),5.44(s,2H),2.26(s,3H),2.10(s, 3H).$^{13}$CNMR(101MHz,CDCl3)δ198.1,167.3,148.9,137.6,137.2,133.5,131.7,130.4,125.9,124.9,122.4,115.0,112.61,109.0,87.9,76.1,71.1,64.0,19.6,12.9.ESI-HRMS(m/z):calcd.for$C_{24}H_{17}NCo_2NaO_8$[M+Na]$^+$: 587.9516; found 587.9506.

Complex **3**:301.6 mg was obtained as red powder. Yield: 52.1%. Ethyl acetate/hexane (1:6); Rf=0.36.IR (KBr disk, $cm^{-1}$): 2094vs, 2050vs, 2032vs, 2016vs, 2002vs (Co-CO), 1735s, (COO). $^{1}$H NMR (400 MHz, Chloroform-*d*) δ 7.72 (d, *J* = 9.3 Hz, 3H), 7.65 – 7.58 (m, 1H), 7.56 – 7.46 (m, 2H), 7.42 (t, *J* = 8.6 Hz, 2H), 7.19 (s, 1H), 5.95 (s, 1H), 5.39 – 5.01 (m, 2H), 3.88 – 3.70 (m, 1H), 1.60 – 1.45 (m, 3H). $^{13}$C NMR (101 MHz, CDCl3) δ199.4, 196.5, 173.6, 140.6, 138.0, 137.5, 132.5, 131.6,130.5, 129.2, 129.1,128.6, 128.3, 77.2, 71.97, 65.72, 45.32, 18.48.ES I-HRMS (m/z): calcd. for $C_{25}H_{16}NaCo_2O_9$ [M+Na]$^+$: 600.9356; found 600.9348.

Complex **4**: 396.6 mg was obtained as red powder. Yield: 58.4%. Ethyl acetate/hexane (1:5);Rf=0.36.IR (KBr disk, $cm^{-1}$): 2096vs, 2063vs, 2034vs, 2010vs (Co-CO), 1720s (COO). $^{1}$H NMR (400 MHz, Chloroform-*d*) δ 7.76 – 7.48 (m, 4H), 7.21 (s, 1H), 7.14 (s, 1H), 6.82 (dd, *J* = 8.9, 2.4 Hz, 1H), 6.50 (td, *J* = 8.8, 2.5 Hz, 1H), 5.96(s,1H),5.26(s,2H)3.56(s,2H),2.78(s,3H),2.16(s,3H).$^{13}$CNMR(101MHz,Chloroform-*d*)δ197.9,170.8,162.1,147.2,145.1,141.9,136.3,130.1,129.4,127.7,125.5,123.5,112.2,71.7,65.2,54.7.ESI-HRMS (m/z): calcd. for $C_{29}H_{20}Fco_2O_9S$ [M+H]$^+$:680.9476; found 680.9558.

Complex **5**: 302.6 mg was obtained as red powder. Yield: 53.4%. Ethyl acetate/hexane (1:4); Rf=0.44 IR (KBr disk, $cm^{-1}$): 2098vs, 2051vs, 2037vs, 2026vs (Co-CO), 1736s (COO). $^{1}$H NMR (400 MHz, Chloroform-*d*) δ 7.46 (d, *J* = 7.5 Hz, 2H), 7.37 (t, *J* = 7.7 Hz, 2H), 7.32 (s, 1H), 7.19 (s, 1H), 7.08 (t, *J* = 11.0 Hz, 2H), 5.96 (s, 1H), 5.48 – 5.01 (m, 2H), 3.76 (q, *J* = 7.4, 7.0 Hz, 1H), 1.51 (d, *J* = 6.2 Hz, 3H).$^{13}$CNMR(101MHz,Chloroform-*d*)δ205.9,172.7,159.9,140.4,134.5,129.9,129.8,127.9,127.4,126.6,122.6,114.4,114.2,76.2,70.9,64.7,43.9.ESI-HRMS(m/z):calcd.for$C_{24}H_{15}FCo_2NaO_8$ [M+Na]$^+$: 590.9313; found 590.9308. calcd. for $C_{24}H_{15}Co_2FKO_8$[M+K]$^+$: 606.9052; found 606.9057.

Complex **6**: 302.1mg was obtained as red powder. Yield: 51.6%. Ethyl acetate/hexane (1:5); Rf=0.44. IR (KBr disk, $cm^{-1}$): 2098vs, 2060vs, 2034vs, 2021vs, 1998vs(Co-CO),1690s(COO).$^{1}$HNMR(400MHz,Chloroform-*d*)δ9.90(s,1H),8.27(s,2H),7.83(s,1H),7.09(s,2H),6.64(s,1H),6.08(s,1H),5.48(s,2H),2.33(s,3H).$^{13}$CNMR(101MHz,Chloroform-*d*)δ198.0,166.3,155.7,152.7,139.1,138.2,133.8,127.9,125.6,124.0,121.1,112.4,105.4,87.1,71.1,64.8,14.0.ESI-HRMS(m/z):calcd.for$C_{22}H_{14}ClCo_2N_2O_8$

$[M+H]^+$: 586.9163; found 586.9133. calcd. for $C_{22}H_{13}ClCo_2N_2NaO_8$ $[M+Na]^+$: 608.8922; found 608.8957.

Complex **7**: 336.6mg was obtained as red powder. Yield: 54.2%. Ethyl acetate/hexane (1:5); Rf=0.40. IR (KBr disk, $cm^{-1}$): 2097vs, 2045, 2012 vs, (Co-CO), 1682s (COO). $^1$H NMR (400 MHz, Chloroform-*d*) δ 9.52 (s, 1H), 8.01 (d, *J* = 8.0 Hz, 1H), 7.44 – 7.19 (m, 6H), 6.74 (t, *J* = 7.6 Hz, 1H), 6.07 (s, 1H), 5.44 (s,2H).$^{13}$CNMR(101MHz,Chloroform-*d*)δ205.9,167.0,146.1,140.4,133,6,131.0,130.7, 128.9,123.4,118.7,117.3,113.2,76.2,71.2,64.4.ESI-HRMS(m/z):calcd.For$C_{23}H_{12}F_3Nco_2NaO_8$ $[M+Na]^+$: 627.9077; found 627.9067.

Complex **8**: 268.6mg was obtained as red powder. Yield: 47.2%. Ethyl acetate/hexane (1:5); Rf=0.35.IR (KBr disk, $cm^{-1}$): 2098vs, 2056vs, 2034vs, 2019vs (Co-CO), 1715s (COO). $^1$H NMR (400 MHz, Chloroform-*d*) δ： 8.49 (s, 1H), 8.11 (s, 1H), 7.92 (s, 1H), 7.38 (s, 1H), 6.05 (s, 1H), 5.46 (s, 2H), 1.27 (s, 12H). $^{13}$C NMR (101MHz,Chloroform-*d*)δ： 198.0, 165.4, 138.3, 135.2, 131.2, 126.8, 76.1, 71.0, 64.4,23.8.ESI-HRMS(m/z):calcd.for $C_{22}H_{19}Bco_2NaO_{10}$ $[M+Na]^+$: 594.9633; found 594.9664.

Complex **9**: 316.2mg was obtained as red powder. Yield: 52.6%. Ethyl acetate/hexane (1:5);Rf=0.38. IR (KBr disk, $cm^{-1}$): 2098vs, 2061vs, 2038vs, 2021vs (Co-CO), 1691s (COO). $^1$H NMR (400 MHz, Chloroform-*d*) δ 10.31 (s, 1H), 8.41 (s, 1H), 8.30 (d, *J* = 7.8 Hz, 1H), 8.00 (s, 1H), 7.83 (d, *J* = 7.8 Hz, 1H), 7.33 (t, *J* = 7.9 Hz, 1H), 7.21 (d, *J* = 7.4 Hz, 1H), 6.73 (dd, *J* = 8.1, 3.1 Hz, 1H), 6.09 (s, 1H), 5.49(s,2H).$^{13}$CNMR(101MHz,Chloroform-*d*)δ206.9,167.2,155.9,153.5,140.2,129.2,1 23.7,119.2,117.3,114.1,76.96,72.2,66.0.ESI-HRMS(m/z):calcd.for$C_{22}H_{11}Co_2F_3N_2NaO_8$ $[M+Na]^+$:628.9029;found 628.9008.

Complex **10**: 320.6mg was obtained as red powder. Yield: 51.8%. Ethyl acetate/hexane (1:5);Rf=0.33 IR (KBr, $cm^{-1}$): 2097vs, 2068vs, 2021vs, 2007, 1996 (Co-CO), 1728s (COO). $^1$H NMR (400 MHz, Chloroform-*d*) δ 7.27 (s, 1H), 7.19 (s, 1H),7.14(d,*J*=7.5Hz,1H),7.06(t,*J*=7.9Hz,1H),6.90(dt,*J*=14.0,7.7Hz,3H),6.49(d,*J*=8.0 Hz,1H),5.98(s,1H),5.28(s,2H),3.82(s,2H).$^{13}$CNMR(101MHz,Chloroform*d*)δ198.2,171 .1,141.1,130.0,128.4,127.9,127.1,123.0,122.9,121.0,117.3,76.20,72.4,,64.8,37.27. ESI-HRMS (m/z): $C_{23}H_{13}Cl_2Co_2NNaO_8$ $[M+Na]^+$: 641.8580; found 641.8542.

Complex **11**: 326.1mg was obtained as red powder.Yield:53.9%. Ethyl acetate/hexane (1:5);Rf=0.44.IR (KBr, $cm^{-1}$): 2099vs, 2056vs, 2033vs, 2006 (Co-CO), 1728s (COO). $^1$H NMR (400 MHz, Chloroform-*d*) δ 7.88 – 7.31 (m, 8H), 5.95 (s, 1H), 5.31(d,*J*=14.2Hz,1H),5.07(d,*J*=14.4Hz,1H),4.78(s,2H),3.74(s,1H),1.49(s,3H).$^{13}$CNM R(101MHz,Chloroform-*d*)δ199,2,174.2,167.5,140.1,138.6,136.3,133.2,132.1,128.4,1 28.3,124.2,122.6,119.7, 88.5 , 71.9 , 65.5 , 50.7 , 44.9 , 18.4.ESI-HRMS (m/z): calcd. for $C_{26}H_{18}NCo_2O_9$ $[M+H]^+$: 605.9646.found 605.9785.

Complex **12**: 306.1mg was obtained as red powder. Yield: 50.9%. Ethyl

acetate/hexane (1:5);Rf=0.46.IR (KBr, $cm^{-1}$): 2098vs, 2057vs, 2025vs (Co-CO) $^{1}H$ NMR (400 MHz, Chloroform-*d*) δ 7.81 (d, *J* = 8.2 Hz, 2H), 7.43 (d, *J* = 8.3 Hz, 2H), 7.19(s,1H),7.10(s,2H),7.04(d,*J*=7.9Hz,2H),6.67(s,1H),5.88(s,1H),4.26(d,*J*=6.5Hz,2H),2.32(s,3H).$^{13}$CNMR(101MHz,Chloroform-*d*)δ197.4,141.8,138.8,138.4,128.8,127.7,127.1,124.7,124.6,105.5,76.19,71.52,45.0,20.3.ESI-HRMS:calcd.for$C_{26}H_{17}F_3Co_2N_3O_8S$[M+H]$^+$705.9352,found705.9355, calcd. for $C_{26}H_{16}F_3Co_2N_3NaO_8S$[M+Na]$^+$ 727.9172, found 727.9169.

Complex **13**: 455.2.1mg was obtained as red powder.Yield:61.9%. Ethyl acetate/hexane (1:6);Rf=0.42. IR (KBr, $cm^{-1}$): 2096vs, 2058vs, 2021vs (Co-CO). $^{1}H$ NMR (400 MHz, Chloroform-*d*) δ 7.98 (dd, *J* = 8.6, 2.4 Hz, 1H), 7.73 (d, *J* = 8.7 Hz, 1H), 7.65 (d, *J* = 2.4 Hz, 1H), 7.48 (t, *J* = 7.8 Hz, 2H), 7.26 (s, 1H), 7.06 (d, *J* = 7.9 Hz,2H),5.82(s,1H),5.22(s,2H),3.05(s,3H).$^{13}$CNMR(101MHz,Chloroform-*d*)δ207.0,153.8,148.3,134.7,133.7,130.9,126.3,119.9,117.8,112.3,77.3,72.9,52.6,40.0.ESI-HRMS: calcd.for$C_{22}H_{14}Co_2N_2NaO_{11}S$[ M+$Na^+$ ]$^+$654.8880, found 654.8926.

Complex **14**: 325.1mg was obtained as red powder.Yield:60.9%. Ethyl acetate/hexane (1:8); Rf=0.36. IR (KBr, $cm^{-1}$): 2099vs, 2056vs, 2034vs, 2014vs (Co-CO). $^{1}H$ NMR (400 MHz, Chloroform-*d*) δ 7.56 (d, *J* = 15.9 Hz, 1H), 7.02 (d, *J* = 10.8 Hz, 2H), 6.85 (d, *J* = 8.3 Hz, 1H), 6.26 (d, *J* = 15.9 Hz, 1H), 5.98 (s, 1H), 5.24 (s, 2H),4.19(q,*J*=7.2Hz,2H),3.78(s,3H),1.27(t,*J*=7.2Hz,3H).$^{13}$CNMR(101MHz,Chloroform-*d*)δ198.1,166.2,149.1,148.5,143.4,127.4,121.0,115.3,112.7,109.5,87.5,71.3,68.2,59.4,54.7,13.3.ESI-HRMS(m/z):calcd.for$C_{21}H_{17}Co_2O_{10}$[M+H]$^+$: 546.9486; found 546.9461.

Complex **15**: 455.2.1mg was obtained as red powder. Yield: 61.9%. Ethyl acetate/hexane (1:10); Rf=0.38.IR (KBr, $cm^{-1}$): 2098vs, 2062vs, 2035vs, 2023 (Co-CO), 1712s (COO). $^{1}H$ NMR (400 MHz, Chloroform-*d*) δ 8.02 (d, *J* = 8.4 Hz, 2H),7.88(d,*J*=8.8Hz,2H),7.42(d,*J*=8.6Hz,2H),7.30(d,*J*=8.4Hz,2H),7.19(s,2H),6.79(s,1H),5.96(s,1H),5.26(s,2H).$^{13}$CNMR(101MHz,Chloroform-*d*)δ198.3,168.3,155.1,149.2,145.5,143.1,131.3,129.2,127.4,120.3,87.7,64.2,54.6.ESI-HRMS:calcd.for$C_{26}H_{15}F_3Co_2N_3O_{10}S$[M+H]$^+$735.9004,found735.9267,calcd.for$C_{26}H_{14}F_3Co_2N_3NaO_{10}S$[M+Na]$^+$757.8914, found 757.9084.

### 4.3 Crystallographic analysis

Crystallographic analysis Diffraction data were collected at 291 K on a Bruker Smart Apex II diffractometer with Mo-Ka radiation (k = 0.71070 A ° ) using a SMART CCD camera. Diffractometer control, data collection and initial unit cell determination were performed using ‘‘SMART.’’ Frame integration and unit cell refinement were carried out with the ‘‘SAINT’’ software package. Absorption corrections were applied with SADABS (v 2.10 Sheldrick). Structureswere solved by direct methods using SHELXS-97 and refined by full-matrix least-squares using

SHELXL-97 [43]. All nonhydrogen atoms were refined anisotropically. Hydrogen atoms attached to the nitrogen of amino groups were located in the electron difference map, and remaining hydrogen atoms were placed using a ‘‘riding model’’ andincluded inthe refinement at calculated positions. CCDC 1820688 (9), 1820689(11), 1820690(14) and 1820687 (16) contain the supplementary crystallographic data for this paper.

**4.4. Lipophilicity (log P o/w)**

The lipophilicity of complex was determined using the flaskshaking method where n-octanol and 0.1 M PBS were used as the organic and aqueous phase respectively. n-Octanol was presaturated with 0.1 M PBS by swirling at 45 rpm for 24 h. The tested complex was dissolved in the isolated organic phase at a concentration of 50 uM. An equal volume of aqueous PBS was added, and the mixture was swirled for 8 h at 45 rpm at 37□. The solution was then centrifuged, and the amounts of complex in both layers were determined by ICP-AES.

**4.5 CO-release tests with myoglobin assay**

The release of CO from the metal carbonyl complexes was studied spectrophotometrically by measuring the conversion of deoxy-myoglobin (deoxy-Mb) to carbonyl myoglobin (Mb-CO). The amount of Mb-CO formed was quantified by measuring the absorbance at 540 nm. A stock solution of myoglobin (lyophilised horse heart) (60 μM final concentration) was prepared fresh by dissolving the protein in phosphate buffered saline (PBS, 0.1M, pH=7.4). Sodium dithionite (0.1%) was added to convert the myoglobin stock to deoxy-Mb. A 2 ml quantity of this solution was assayed to obtain a deoxy-Mb spectrum and then bubbled with CO to get an Mb-CO spectrum. Each complex was dissolved in water and added to deoxy-Mb in the cuvette, mixed using a pipette and then overlaid with 500 μL light mineral oil to prevent CO escaping or the myoglobin being oxygenated. This is the standard procedure; other experiments have been undertaken using different concentrations of myoglobin.

In these experiments, the absorption peak of deoxy-Mb at 560 nm was replaced by the two peaks of Mb-CO at 540 and 578 nm. The concentration of myoglobin in the stock solution was calculated from the absorption maximum of the Mb-CO solution at 540 nm.

**4.6 Cytotoxicity assays**

Hela cell, HepG2 cell, MCF-7 cell, A549 cell, HT-29 cell and W138 cells line were purchased from cell resources Center for Shanghai Life Science Institute of Chinese Academy of Sciences (China). The cells were cultivated at 37 °C, 10% $CO_2$, 100% humidity in RPMI1640 medium, enriched with glucose and supplemented with

10 % fetal bovine serum, non-essential amino acids, antibiotics (penicillin/ streptomycin) and antifungals.Typically, 8 μmol of the complex was dissolved in 1.0 mL of culture medium with vigorous stirring. Growth inhibitory effect toward the cell line was determined by means of MTT colorimetric assay. The cells (100 μL, $1\times10^5$cells $mL^{-1}$) were seeded into 96-well plates and left to adhere for 24h. The media was removed from the wells and replaced with fresh media containing the complexes with different concentrations (6.5, 12.5, 25, 50, 100, 200, 400 and 800 μmol $L^{-1}$), respectively. The cells were then incubated for another 24 h before the incubation media were replaced with the complete medium and MTT (10 μL, 5 mg $mL^{-1}$ in phosphate buffer solution, PBS) was added to each well of the plate. The cells were further incubated for 4 h before the media were replaced with DMSO (100 μL). Absorbance at 490 nm for each well of the plates was recorded with a microplate reader. In the MTT assay, DMSO (100 μL) in a well was used as blank and cells in the well without the addition of any complexes were taken as a control (100 % in cell viability).

**4.7 Bicinchoninic acid (BCA) protein assay**

In order to exclude the influence of the total amount of protein on the determination of the following cytokine levels, protein quantification of each protein was carried out using BCA protein Assay. Briefly, samples were removed and placed into a 96-well plate (20μL per well). BCA reagent A and reagent B were formulated as working solutions, which was added to each well (200μL per well) and left to react for 0.5 h in 37℃. And then the plate was shaken for 10 min and the absorbance read at 562 nm on a microplate reader. The concentration of protein in each sample was calculated from a standard curve generated with standard solution.

**4.8 Determination of COX-2 levels**

The level COX-2 in each sample was determined using a commercially available kit from Shanghai MLBIO Biotechnology Co.Ltd. The assay was performed according to the manufacturers' instructions. Briefly, cell were collected from 6-well plate immediately after lysed by RIPA Lysis Buffer and spun at 12,000×g for 10 min to remove any particulates. Each protein solution was measured by BCA Protein Assay Kit. The protein solution for concentration of 0.1mg ml-1 was added to a 96-well plate precoated with affinity-purified polyclonal antibodies specific for the mouse of our cytokines. An enzyme-linked polyclonal antibody specific for the mouse of our cytokines was added to the wells and left to react for 0.5 h followed by a final wash to remove any unbound antibody-enzyme reagent. The intensity of the color detected at 450 nm was measured after addition of chromogen solution A, B and stop solution and was proportional to the amount of four cytokines produced. The COX-2

levels which in each sample was calculated from a standard curve generated with standard solution.

4.9 **Myocardial protective effects of the complexes**

The rat cardiac H9c2 cells were purchased from the Cell Bank of the Chinese Academy of Sciences (Shanghai,China) and cultured in DMEM supplemented with 10% FBS,100 U•mL-1 of penicillin, and 100 μg•mL-1 of streptomycin at 37 °C in a humidified atmosphere of 5% $CO_2$ .Cardiomyocyte survival rate .The H9c2 cells were cultured in 96 - well plates at a density of $5 \times 10^4$ cells /mL and cultured for 8 h at 37 ℃ and 5 % $CO_2$ incubator for 8 hours. The tests were divided into blank group, $H_2O_2$ group, complex（10μM、25μM、50μM）-$H_2O_2$ group. $H_2O_2$ was 400μM, and the control group only added cells without drugs. The cells survival rate was detected after 24h. After cells were treated with $H_2O_2$ for 1h, 4h and 8h, respectively, the culture medium was discarded and the $H_2O_2$ group was supplemented with fresh medium. Then the cell viability was measured after 24 hours of incubation.

Assays for enzyme activities The H9c2 cells were cultured in 6-well plates overnight and then treated with $H_2O_2$ (400μM) for another 1h. The activities of SOD and the MDA content were measured using commercial kits following the manufacturer's instruction (NanJing JianCheng Bioengineering Institute, Nanjing, China).

**4.10 Antihypertensive effect in SHR**

A total of 40 male clean spontaneously hypertensive rats (SHR) were divided into normal control group, captopril group (10 mg $kg^{-1}$), nifedipine nifelat group (10 mg. $kg^{-1}$) and compound group (10, 20, 40 mg. $kg^{-1}$) by randomized block design. Male WKY rats were used as the normal control group. All the drugs and compounds were administered by intraperitoneal injection as a 2mL/kg. The solvent was the mixed solution of 0.5% sodium carboxymethyl cellulose and DMSO (v/v 3:1). The control group and WKY group were injected mixed solution without containing compound or drug. Tail blood pressure and heart rate were measured before administration. After administration, blood pressure and heart rate were measured every 10min, lasting for 3 h. The arterial systolic pressure, diastolic arterial pressure (DBP) and heart rate were recorded before and after administration.

Method of measurement: In a brief, in a quiet state of consciousness, the rats were fixed to a special fixture. The rat tail was covered until the roots by pressure cuff, which strapped pulse transducer to contact closely to the ventral tail artery. When the rat pulse wave stabilized, it began to measure. The pressure cuff was inflated and pressurized until the blocking pressure was 250 mmHg. (The pulse wave disappeared when the pressure reached the systolic pressure level.) After the pressure maintains 6

seconds, it slowly decompresses. When the first pulse waves appear, the corresponding blood pressure is the arterial systolic pressure, the peak of the corresponding curve is the arterial diastolic pressure, and the system automatically displays the heart rate. Each group was continuously measured 6 times. All data are expressed as the mean ± standard error (SE); n refers to number of animals studied in each group. Significance was accepted at $P < 0.05$.

**Conflict of Interest**

The authors confirm that this article content has no conflict of interest.

**Acknowledgements**

This work was financially supported by the National Natural Science Foundations of China (no. 21171079) and the Recruitment Program of Global Experts (1000 Talents Plan).

**References**

[1]Johnson T R, Mann B E, Clark J E, et al. Metal carbonyls: a new class of pharmaceuticals? [J]. Angewandte Chemie International Edition, 2003, 42(32): 3722-3729.

[2] Motterlini R, Otterbein L E. The therapeutic potential of carbon monoxide[J]. Nature reviews Drug discovery, 2010, 9(9): 728.

[3]Ahmad, Shakil, et al. "Carbon monoxide inhibits sprouting angiogenesis and vascular endothelial growth factor receptor-2 phosphorylation." *Thrombosis and haemostasis* 114.02 (2015): 329-337.

[4] Wegiel, Barbara, et al. "Carbon monoxide expedites metabolic exhaustion to inhibit tumor growth." *Cancer research* 73.23 (2013): 7009-7021.

[5]Simon, Thomas, Ignacio Anegon, and Philippe Blancou. "Heme oxygenase and carbon monoxide as an immunotherapeutic approach in transplantation and cancer." *Immunotherapy* 3.4s (2011).

[6]Motterlini R, Mann B E, Johnson T R, et al. Bioactivity and pharmacological actions of carbon monoxide-releasing molecules[J]. Current pharmaceutical design, 2003, 9(30): 2525-2539.

[7]Clark J E, Naughton P, Shurey S, et al. Cardioprotective Actions by a Water-Soluble Carbon Monoxide–Releasing Molecule[J]. Circulation Research, 2003, 93(2):2-8.

[8] Motterlini R, Sawle P, Hammad J, et al. Vasorelaxing effects and inhibition of nitric oxide in macrophages by new iron-containing carbon monoxide-releasing molecules (CO-RMs).[J]. Pharmacological Research the Official Journal of the Italian Pharmacological Society, 2013, 68(1):108.

[9] Crook S H, Mann B E, Meijer A J H M, et al. [Mn(CO) {S CNMe(CH CO H)], a new water-soluble CO-releasing molecule[J]. Dalton Transactions, 2011, 40(16):4230-4235.

[10] Atkin A J, Williams S, Sawle P, et al. Mu2-alkyne dicobalt(0)hexacarbonyl complexes as carbon monoxide-releasing molecules (CO-RMs): probing the release mechanism[J]. Dalton Trans,

2009, 19(19):3653-3656.

[11] Nobre L S, Seixas J D, Romão C C, et al. Antimicrobial Action of Carbon Monoxide-Releasing Compounds[J]. Antimicrobial Agents & Chemotherapy, 2007, 51(12):4303.

[12]Ott I, Schmidt K, Kircher B, et al. Antitumor-active cobalt-alkyne complexes derived from acetylsalicylic acid: studies on the mode of drug action. *J Med Chem*. 2005, *48*(2): 622-629.

[13]Sydonie D. Schimler, David J. Hall, Stefan L. Debbert. Anticancer (hexacarbonyldicobalt) propargyl arylethers: Synthesis, anti-proliferative activity, apoptosis induction, and effect on cellular oxidative stress. *J Inorg Biochem.* 2013, *119*, 28–37.

[14]Kathrin Schmidt, Manfred Jung, Roland Keilitz, Beate Schnurr, Ronald Gust Acetylenehexacarbonyldicobalt complexes, a novel class of antitumor drugs. *Inorganica Chim Acta*.2000, 306, 6–16.

[15]S.Top, A. Vessie`res, G.J. Jaouen, Synthetic strategy for organometallic complexes of rhenium with exceptionally high affinity for the oestradiol receptor; their potential use as imaging and therapeutic agents. *J. Chem. Soc. Chem. Commun*.

[16]Sawle, Philip, et al. "Carbon monoxide‐releasing molecules (CO‐RMs) attenuate the inflammatory response elicited by lipopolysaccharide in RAW264. 7 murine macrophages." *British journal of pharmacology* 145.6 (2005): 800-810.

[17]Lee, Wen-Ying, et al. "The induction of heme oxygenase-1 suppresses heat shock protein 90 and the proliferation of human breast cancer cells through its byproduct carbon monoxide." *Toxicology and applied pharmacology* 274.1 (2014): 55-62.

[18] Gong, Yaguo, et al. "Synthesis, toxicities and cell proliferation inhibition of CO-releasing molecules containing cobalt." *Transition Metal Chemistry* 40.4 (2015): 413-426.

[19] Hanahan D, Weinberg R A. The hallmarks of cancer[J]. cell, 2000, 100(1): 57-70.

[20]Hanahan D, Weinberg R A. Hallmarks of cancer: the next generation[J]. cell, 2011, 144(5): 646-674.

[21]Siironen, Päivi, et al. "VEGF-C and COX-2 expression in papillary thyroid cancer." *Endocrine-Related Cancer* 13.2 (2006): 465-473.

[22]Erkanli, Serkan, et al. "COX-2 and survivin are overexpressed and positively correlated in endometrial carcinoma." *Gynecologic oncology* 104.2 (2007): 320-325.

[23]Matsumoto, Gaku, et al. "Tumor size significantly correlates with postoperative liver metastases and COX-2 expression in patients with resectable pancreatic cancer." *Pancreatology* 7.2 (2007): 167-173.

[24]Ahnen D J. Colon cancer prevention by NSAIDs: what is the mechanism of action?[J]. European Journal of Surgery, 1998, 164(S12): 111-114.

[25]Thun M J, Henley S J, Patrono C. Nonsteroidal anti-inflammatory drugs as anticancer agents: mechanistic, pharmacologic, and clinical issues[J]. Journal of the National Cancer Institute, 2002, 94(4): 252-266.

[26]Herendeen J M, Lindley C. Use of NSAIDs for the chemoprevention of colorectal cancer[J]. Annals of Pharmacotherapy, 2003, 37(11): 1664-1674.

[27]Rao C V, Reddy B S. NSAIDs and chemoprevention[J]. Current cancer drug targets, 2004, 4(1): 29-42.

[28]Gurpinar E, Grizzle W E, Piazza G A. NSAIDs inhibit tumorigenesis, but how?[J]. Clinical Cancer Research, 2014, 20(5): 1104-1113.

[29]Guadagni F, Ferroni P, Palmirotta R, et al. Non-steroidal anti-inflammatory drugs in cancer prevention and therapy[J]. Anticancer research, 2007, 27(5A): 3147-3162.

[30]Gupta R A, DuBois R N. Colorectal cancer prevention and treatment by inhibition of cyclooxygenase-2[J]. Nature Reviews Cancer, 2001, 1(1): 11-21.

[31]DuBois R N, Smalley W E. Cyclooxygenase, NSAIDs, and colorectal cancer[J]. Journal of gastroenterology, 1996, 31(6): 898-906.

[32]Duffy C P, Elliott C J, O'Connor R A, et al. Enhancement of chemotherapeutic drug toxicity to human tumour cells in vitro by a subset of non-steroidal anti-inflammatory drugs (NSAIDs)[J]. European Journal of Cancer, 1998, 34(8): 1250-1259.

[33]De Groot D J A, De Vries E G E, Groen H J M, et al. Non-steroidal anti-inflammatory drugs to potentiate chemotherapy effects: from lab to clinic[J]. Critical reviews in oncology/hematology, 2007, 61(1): 52-69.

[34]Kim K S, Yoon J H, Kim J K, et al. Cyclooxygenase inhibitors induce apoptosis in oral cavity cancer cells by increased expression of nonsteroidal anti-inflammatory drug-activated gene[J]. Biochemical and biophysical research communications, 2004, 325(4): 1298-1303.

[35]Kim K S, Yoon J H, Kim J K, et al. Cyclooxygenase inhibitors induce apoptosis in oral cavity cancer cells by increased expression of nonsteroidal anti-inflammatory drug-activated gene[J]. Biochemical and biophysical research communications, 2004, 325(4): 1298-1303.

[36]Woo D H, Han I S, Jung G. Mefenamic acid-induced apoptosis in human liver cancer cell-lines through caspase-3 pathway[J]. Life sciences, 2004, 75(20): 2439-2449.

[37]Klampfer L, Cammenga J, Wisniewski H G, et al. Sodium salicylate activates caspases and induces apoptosis of myeloid leukemia cell lines[J]. Blood, 1999, 93(7): 2386-2394.

[38]Li M, Wu X, Xu X C. Induction of apoptosis in colon cancer cells by cyclooxygenase-2 inhibitor NS398 through a cytochrome c-dependent pathway[J]. Clinical cancer research, 2001, 7(4): 1010-1016.

[39]Duncan K, Uwimpuhwe H, Czibere A, et al. NSAIDs induce apoptosis in nonproliferating ovarian cancer cells and inhibit tumor growth in vivo[J]. IUBMB life, 2012, 64(7): 636-643.

[40]Gong, Yaguo, et al. "Toxicity, bio-distribution and metabolism of CO-releasing molecules based on cobalt." *Free Radical Biology and Medicine* 97 (2016): 362-374.

[41] Clark J E, Naughton P, Shurey S, et al. Cardioprotective actions by a water-soluble carbon monoxide-releasing molecule.[J]. Circulation Research, 2003, 93(2):2-8.

[42] Durante W. Carbon monoxide and bile pigments: surprising mediators of vascular function[J]. Vascular Medicine, 2002, 7(3): 195-202.

[43]Sheldrick G M. A short history of SHELX[J]. Acta Crystallographica Section A: Foundations of Crystallography, 2008, 64(1): 112-122.

Highlights

►Synthesize a series of carbonyl cobalt CORMs with selectively inhibiting cyclooxygenase-2.

►Evaluate anti-tumor activities and cyclooxygenase-2 inhibition in tumor cells.

►Investigate the protective effect of complex on oxidative damage of rat myocardial H9c2 cells and the antihypertensive effect in SHR.